Handbook of Hydrology,
Ed. R. Maidment,
McGraw-Hill Book Company,
New York, 1992

CHAPTER 10
FLOW ROUTING

D. L. Fread
Director, Hydrologic Research Laboratory
National Weather Service, NOAA

10.1 INTRODUCTION

10.1.1 General

Flow routing is a mathematical procedure for predicting the changing magnitude, speed, and shape of a flood wave as a function of time (i.e., the **flow hydrograph**) at one or more points along a **watercourse** (waterway or channel). The watercourse may be a river, stream, reservoir, estuary, canal, drainage ditch, or storm sewer. The flow hydrograph (**unsteady flow**) can result from precipitation runoff (rainfall and/or snowmelt), reservoir releases (spillway, gate, and turbine releases and/or dam failures), landslides into reservoirs, or tides (astronomical and/or wind-generated storm surges).

Many ways have been sought to predict the characteristic features of a flood wave in order to determine necessary actions for protecting life and property from the effects of flooding, and to improve the transport of water through natural or man-made watercourses for economic reasons. Commencing with investigations as early as the 17th century, mathematical techniques for flow routing have continually evolved over time. In 1871, Barré de Saint-Venant (116) formulated the basic theory for one-dimensional analysis of unsteady flow; however, due to the mathematical complexity of the **Saint-Venant equations**, simplifications were necessary to obtain feasible solutions for the important characteristics of a flood wave and its movement. This resulted in the gradual development of many simplified flow routing methods. Only within the last four decades could the complete Saint-Venant equations be solved via computers with varying degrees of feasibility.

Flow routing may be classified as either lumped or distributed. In **lumped flow routing** or **hydrologic routing**, the flow is computed as a function of time at one location along the watercourse; however, in **distributed flow routing** or **hydraulic routing**, the flow is computed as a function of time simultaneously at several cross sections along the watercourse (see Fig. 10.1.1). Two methods for lumped flow routing and two for distributed flow routing are presented herein along with their data requirements. Chapter 10 concludes with several complexities which can be encountered in channel flow routing.

10.1.2 Routing Model Selection

Flow routing has been an important type of hydrologic analysis, and its inherent complexity and computational requirements have resulted in the development of many routing models. The literature abounds with a wide spectrum of useable flow routing models (44,88,94,95), which are sufficiently accurate when used within the bounds of their limitations. Selection of a flow routing model for a particular application is influenced by the relative importance placed on the following factors: (a) the model provides appropriate hydraulic information to answer the

user's questions; (b) the model's accuracy; (c) the accuracy required in the flow routing application; (d) the type and availability of required data; (e) available computational facilities and costs; (f) familiarity with a given model; (g) extent of documentation, range of applicability, and availability of a "canned" or packaged routing model; (h) complexity of the mathematical formulation if the routing model is to be totally developed from "scratch" (coded for computer); and (i) capability and time available to develop a particular type of routing model. Taking the above factors into consideration and recognizing that the relative importance of each may change depending on the application, it is apparent there is no universally superior flow routing model; and a judicious selection of a model from among the several available models is necessary. The simplified routing models are appealing due to their computational simplicity; however, accuracy considerations can restrict their range of applicability.

Accuracy of Reservoir Routing Models. In reservoir applications, the accuracy of **level-pool routing** models (see Section 10.2.2) relative to the more accurate distributed **dynamic routing** models (see Section 10.3.3) is shown in Fig. 10.1.2, an extension of the author's previous work on this subject (50). The error (in percent) associated with level-pool routing is expressed as a normalized error for the rising limb of the outflow hydrograph. The peak outflow is used as the normalizing parameter. The normalized error (E_q) is:

$$E_q = \frac{100}{Q_{D_p}} \sqrt{\frac{\sum_{i=1}^{N'} \left(Q_{L_i} - Q_{D_i}\right)^2}{N'}} \qquad (10.1.1)$$

in which Q_{L_i} is the level-pool routed flow; Q_{D_i} is the dynamic routed flo Q_{D_p} is the dynamic routed flow peak, and N' is the number of computed discharges comprising the rising limb of the routed hydrograph. Since level-pool routing is based on the assumption of a horizontal water surface along the length of the reservoir at all times, the error (E_q) associated with level-pool routing increases as (a) reservoir mean depth (D_r) decreases, (b) reservoir length (L_r) increases, (c) time of rise (T_r) of inflow hydrograph decreases, and (d) inflow hydrograph volume decreases. These effects can be represented by three dimensionless parameters, i.e., $\sigma_\ell = D_r/L_r$, $\sigma_t = L_r/(3600\ T_r \sqrt{g\ D_r})$ in which g is the gravity acceleration constant and T_r is the time (hrs) from beginning of rise until the peak of the hydrograph, and σ_v = hydrograph volume/reservoir volume. As shown in Fig. 10.1.2, E_q increases as σ_t increases and as σ_ℓ and σ_v decrease; also the influence of σ_v increases as σ_ℓ decreases.

Accuracy of River Routing Models. In river routing applications, the lumped as well as the kinematic-type and diffusion-type routing models offer the advantage of simplicity where there is an absence of significant backwater effects. Accuracy considerations restrict these models to applications where the depth-discharge relation is essentially single-valued, and the product of the time of rise of the hydrograph and the channel bottom slope is not small. An approximate criterion (42,107) which restricts kinematic-type routing relative to dynamic routing models errors to less than E (percent) is:

$$E < \mu' \phi n^{1.2} q_p^{0.2}/(T_r S_o^{1.6}) \quad (10.1.2)$$

The error term (E), expressed in percent, represents the energy slope ratio of kinematic models to dynamic models. A similar criterion (E') for the diffusion-type routing models is:

$$E' < \mu'' \phi' q_p^{0.4}/(T_r S_o^{0.7} n^{0.6}) \quad (10.1.3)$$

where:

$$\phi = (m+1)^2/(3m+5) \quad (10.1.4)$$

$$\phi' = (m+3)/(3m+5) \quad (10.1.5)$$

in which the units conversion factors (μ') is 0.21 (US units) or 0.43 (SI units) and (μ'') is 0.0022 (US units) or 0.0091 (SI units), T_r is the time of rise (hrs) of the inflow hydrograph, S_o is the channel bottom slope (ft/ft), q_p is a unit-width peak discharge (cfs or m^3/s), n is the Manning coefficient for flow resistance, and m is the cross-section shape factor, $0 \leq m \leq 2$, used to describe the channel topwidth B, as $B = ky^m$ in which y is depth of flow (m = 0 for rectangular, m = 0.5 for parabolic, and m = 1.0 for triangular channels).

An inspection of (10.1.2) and (10.1.3) shows the importance of the parameters, T_r and S_o, which can have a large range of possible values. The parameter q_p is not dominant due to the power associated with it, and n has a rather restricted range of possible values, say 0.015 to 0.25. It is also apparent that diffusion models are applicable for a wider range of bottom slopes and hydrographs than the kinematic models. The simple diffusion-type Muskingum-Cunge method (see Section 10.3.2) can be used effectively in many applications where (10.1.3) is satisfied and backwater effects or reverse flows can be neglected.

In cases involving a gently sloping channel and rapidly rising flood wave, when the combination of S_o and T_r becomes small enough that (10.1.3) cannot be satisfied, dynamic routing models (see Section 10.3.3) based on the complete one-dimensional Saint-Venant equations are required. Dynamic routing models are required for (a) slowly rising flood waves in mild sloping channels i.e., slopes less than about 0.10 percent; (b) situations where backwater effects are important due to tides, significant tributary inflows, natural constrictions, dams, and/or bridges; and (c) situations where waves propagate upstream from large tides and storm surges or very large tributary inflows. As the trend for increased computer computational speed and storage capabilities at decreased costs continues, the economic feasibility of using dynamic routing models for a wider range of applications will increase, since dynamic models have the capability to correctly simulate the widest spectrum of wave types and waterway characteristics. Implicit dynamic routing models -- the most efficient and versatile although the most complex of the dynamic routing models -- will be increasingly utilized as improvements continue to be made in their computational robustness and reliability.

10.2 LUMPED FLOW ROUTING

10.2.1 General

A simplified description of unsteady flow along a watercourse (routing reach) depicts it as a lumped process, as shown in Fig. 10.1.1, in which the **inflow** (I) at the upstream end and the **outflow** (Q) at the end of the watercourse are functions of time, i.e., I(t) and Q(t). The principle of **mass conservation** requires the difference between the two flows (discharges) to be equal to the time rate of change of the storage (S) within the reach, i.e,

$$I(t) - Q(t) = dS/dt \qquad (10.2.1)$$

The **storage** (S) is related to I and/or Q by an arbitrary empirical storage function. The most simple is a single-valued function of outflow (Q), i.e., S = f(Q), or of water-surface elevation (h), i.e., S = f(h). This implies the water surface is level throughout the watercourse, usually a reservoir or lake. A more complex relationship exists for long narrow reservoirs or **open channels** (rivers and streams) where storage is a function of both inflow and outflow.

Solution of (10.2.1) for Q(t) with various approximations for the storage constitutes lumped flow routing. Both graphical and mathematical techniques for solving (10.2.1) have been used. The attractiveness of lumped flow routing is its relative simplicity compared to distributed flow routing. However, lumped flow routing methods for rivers neglect backwater effects and are not accurate for rapidly rising hydrographs routed through mild to flat sloping rivers, and they are also inaccurate for rapidly rising hydrographs in long reservoirs. Lumped flow routing methods (several are listed in Table 10.2.1) can be categorized as: (a) level-pool types which are used for reservoirs, assuming a level water surface at all times, and based on (10.2.1); (b) storage types used for rivers, considering the sloping water surface due to the passage of a flood wave, and are based on (10.2.1); and (c) **linear systems** types which assume the routing channel is composed of linear reservoirs connected by linear channels which may be uniquely characterized by a unit response function, and the inflow (input)-outflow (output) relationship is defined by a convolution integral.

10.2.2 Level-Pool Reservoir Routing

In this technique, the reservoir is assumed always to have a horizontal water surface throughout its length; hence, level-pool. Unsteady flow routing in reservoirs which are not excessively long and in which the inflow hydrograph is not rapidly changing with time, as determined from Fig. 10.1.2, can be approximated by a simple technique known as **level-pool routing.** The water-surface elevation (h) changes with time (t), and the outflow from the reservoir is assumed to be a function of h(t). This is the case for reservoirs with **uncontrolled overflow spillways** such as the ogee-crested, broad-crested weir, and morning-glory types (17,18,19,91). **Gate controlled spillways** can be included in level-pool routing if the gate setting (height of the gate bottom above the gate sill) is a predetermined function of time, since the outflow is a function of h and the extent of gate opening. Several level-pool routing techniques have been proposed, many of them graphical or semigraphical; however, with computerization, nongraphical computational techniques are currently more prevalent. Since

(10.2.1) is an ordinary differential equation, it can be solved by various numerical techniques such as a Runge-Kutta method (19) or an **iterative trapezoidal integration method** (40,45) which is presented herein.

Iterative Trapezoidal Integration Method. In this solution method, the trapezoidal rule is used to integrate the conservation of mass equation (10.2.1). The time domain consists of time lines separated by Δt intervals, i.e., t=0, Δt, $2\Delta t$, ..., $j\Delta t$, $(j+1)\Delta t$. The time rate of change in storage is the product of reservoir surface area (Sa) and change of water-surface elevation (h) over the j^{th} time step, i.e.,

$$dS/dt = 0.5(Sa^j + Sa^{j+1})(h^{j+1} - h^j)/\Delta t^j \qquad (10.2.2)$$

in which the surface area (Sa) is specified as a known tabular function of h. Using average values for I(t) and Q(t) over the Δt interval and substituting (10.2.2) into (10.2.1) yields the following:

$$0.5(I^j+I^{j+1}) - 0.5(Q^j+Q^{j+1}) - 0.5(Sa^j+Sa^{j+1})(h^{j+1}-h^j)/\Delta t^j = 0 \qquad (10.2.3)$$

The inflows (I) at times j and j+1 are known from the specified inflow hydrograph, the outflow (Q) at time j can be computed from the known water-surface elevation (h^j) and an appropriate spillway discharge equation. The surface area (Sa^j) can be determined from the known value of h^j. The unknowns in the equation consist of h^{j+1}, Q^{j+1}, Sa^{j+1}; the latter two are known nonlinear functions of h^{j+1}. Hence, (10.2.3) can be solved for h^{j+1} by an **iterative method** such as **Newton-Raphson**, i.e.,

$$h_{k+1}^{j+1} = h_k^{j+1} - f\left(h_k^{j+1}\right)/f'\left(h_k^{j+1}\right) \qquad (10.2.4)$$

in which k is the iteration counter; and $f\left(h_k^{j+1}\right)$ is the left-hand side of (10.2.3) evaluated with the first estimate for h_k^{j+1}, which for k=1 is either h^j or a linear extrapolated estimate of h^{j+1}; $f'\left(h_k^{j+1}\right)$ is the derivative of (10.2.3) with respect to h^{j+1}. It can be approximated by using a numerical derivative as follows: $f'\left(h_k^{j+1}\right) = \left[f\left(h_k^{j+1}+\varepsilon\right) - f\left(h_k^{j+1}-\varepsilon\right)\right] / \left[\left(h_k^{j+1}+\varepsilon\right) - \left(h_k^{j+1}-\varepsilon\right)\right]$ in which ϵ is a small value, say 0.1 ft (0.03 m). Using (10.2.4), only one or two iterations are usually required to solve (10.2.3) for h^{j+1}. Initially, the pool elevation (h^j) must be known to start the computational process. Once h^{j+1} is obtained, Q^{j+1} can be computed from the spillway discharge equation.

Limitations. As shown in Fig. 10.1.2, level-pool routing is less accurate as reservoir length increases, reservoir mean depth decreases, and time of rise of the inflow hydrograph decreases. This inaccuracy can have significant economic effects on water control management (21,118).

10.2.3 Muskingum River Routing

The **Muskingum method**, developed by McCarthy (92), is a popular lumped flow routing technique in the United States and elsewhere. It assumes a variable discharge/storage equation, i.e.,

$$S = K[X\ I + (1-X)\ Q] \tag{10.2.5}$$

Assuming the stage is a single-valued function of discharge (Q), the storage (S) in the routing reach is represented by (10.2.5) in which the prism storage in the reach is KQ where K is a proportionality coefficient; and, the volume of wedge storage is equal to KX (I-Q), where X is a weighting factor having the range $0 \leq X \leq 0.5$ (most streams have X values between 0.1 and 0.3). The storage beneath a line parallel to the stream bed is called **prism storage;** the water located between this line and the actual profile is **wedge storage.** In a channel, the storage relationship to discharge plots as a single or twisted loop if the storage is assumed to be related only to outflow, i.e., storage is greater for a given outflow during rising stages than during falling stages. This is caused by different backwater profiles existing at various times during passage of the flood wave.

The time rate of change of storage dS/dt in (10.2.1) is represented as follows:

$$dS/dt = (S^{j+1}-S^j)/\Delta t^j = K\left[[X\ I^{j+1}+(1-X)\ Q^{j+1}] - [X\ I^j+(1-X)\ Q^j]\right]/\Delta t^j \tag{10.2.6}$$

where the superscripts j and j+1 denote the times separated by the interval (Δt^j). Substituting (10.2.6) into (10.2.1) yields the following:

$$Q^{j+1} = C_1\ I^{j+1} + C_2\ I^j + C_3\ Q^j \tag{10.2.7}$$

which is the Muskingum flow routing equation, where:

$$C_1 = (\Delta t - 2KX)/[2K(1-X) + \Delta t] \tag{10.2.8}$$

$$C_2 = (\Delta t + 2KX)/[2K(1-X) + \Delta t] \tag{10.2.9}$$

$$C_3 = [2K(1-X) - \Delta t]/[2K(1-X) + \Delta t] \tag{10.2.10}$$

and where $C_1 + C_2 + C_3 = 1$, and $K/3 \leq \Delta t \leq K$ is usually the range for Δt.

Calibration of K and X. Values for K and X can be determined from observed inflow and outflow hydrographs (18,19,91,92,96,122). Using (10.2.6) and the left side of (10.2.1), as expressed in (10.2.3), yields an equation for K, i.e.,

$$K = 0.5\ \Delta t\left[I^{j+1}+I^j-(Q^{j+1}+Q^j)\right]/\left[X(I^{j+1}-I^j) + (1-X)(Q^{j+1}-Q^j)\right] \tag{10.2.11}$$

If at each time interval, values of the numerator are plotted against those of the denominator, a loop is formed. Iteratively varying X will tend to close the loop,

and that value of X which causes the plot to be most nearly a single line is the correct value for the reach. Then K may be computed from the average value determined from (10.2.11) for the correct value of X. Lateral inflows can also be included in the calibration of the Muskingum method (104). If observed inflow and outflow hydrographs are not available to compute K and X, these parameters may be estimated from the hydrograph and river cross-sectional and flow resistance characteristics as shown by Cunge (23) and others (19,32,44,77,94). This technique, known as the **Muskingum-Cunge method**, is best utilized as a distributed routing method and is presented in Section 10.3.2.

Limitations. The Muskingum method sometimes produces unrealistic initial negative dips in the computed hydrograph (23,99); however it provides reasonably accurate results for moderate to slow rising floods propagating through mild to steep sloping watercourses. The Muskingum method is a kinematic-type routing model; it's relative accuracy is approximately defined by (10.1.2). It is not suitable for rapidly rising hydrographs such as dam-break floods, and it neglects variable **backwater effects** due to downstream constrictions, bridges, dams, large tributary inflows, or tidal fluctuations. An index to indicate insignificant backwater effects is: the maximum volume that exceeds the peak normal depth and is stored in backwater pools throughout the routing reach should be insignificant compared to the volume of the rising limb of the inflow hydrograph.

10.3 DISTRIBUTED FLOW ROUTING

10.3.1 General

Unsteady flow in a watercourse is most accurately described as a distributed process because the flow rate, velocity, and depth (elevation) vary in space (at cross sections along the channel) as shown in Fig. 10.1.1. Estimates of these properties in a channel system can be obtained by using distributed flow routing based on the complete differential equations of one-dimensional unsteady flow (the Saint-Venant equations) (116). These equations allow the flow rate and water level to be computed as functions of space and time rather than time alone as in the lumped flow routing methods of Section 10.2. Distributed flow routing based on the complete Saint-Venant equations is known as **dynamic routing.** Also, simplified forms of the Saint-Venant equations, referred to as kinematic and diffusion (zero-inertia) equations, can be used for distributed flow routing.

Saint-Venant Equations. The original **Saint-Venant equations** are the **mass conservation equation**, i.e.,

$$\partial(AV)/\partial x + \partial A/\partial t - q = 0 \qquad (10.3.1)$$

and the **momentum equation**, i.e.,

$$\partial V/\partial t + V\partial V/\partial x + g(\partial h/\partial x + S_f) = 0 \qquad (10.3.2)$$

in which t is time, x is distance along the longitudinal axis of the watercourse, A is cross-sectional area, V is velocity, q is **lateral inflow** or **outflow** distributed along the x-axis of the watercourse (this term was not included in the original derivation), g is the gravity acceleration constant, h is the water-surface elevation above an arbitrary datum such that $\partial h/\partial x = \partial y/\partial x - S_o$ in which

y is the flow depth and S_o is the bottom slope of the watercourse, and S_f is the **friction slope** which may be evaluated using a uniform, steady-flow empirical resistance equation such as Chezy's or Manning's (17,18,19,61,91,96). Equations (10.3.1) and (10.3.2) are quasi-linear, hyperbolic partial differential equations with two dependent parameters (V and h) varying in one dimension only (the x-direction) and two independent parameters (x and t). The area (A) and S_f are known functions of h and/or V. No analytical solutions of the complete equations for most practical applications are available. Derivations of the Saint-Venant equations (61,87,127,129,139) utilize the following basic assumptions: (a) the flow is essentially one-dimensional, (b) the stream length affected by the flood wave is many times greater than the flow depth, (c) the vertical accelerations are negligible and vertical pressure distribution in the wave is hydrostatic, (d) the water density is constant, (e) the channel bed and banks are fixed and not mobile, and (f) the channel bottom slope (S_o) is relatively small, less than about 15 percent.

Application of Distributed Flow Routing. Distributed flow routing models, which compute both the rate of flow (Q) and water-surface elevation (h), are useful for determining floodplain depths, required heights of structures such as bridges or levees, and streamflow velocities affecting the transporting of pollutants. Distributed flow routing models can also be used for such applications as real-time forecasting of river floods, irrigation water deliveries through canals, inundation maps for dam-break contingency planning, transient waves created in reservoirs by gate or turbine changes, landslide-produced waves in reservoirs, and unsteady flow in storm sewer systems. The true flow process in each of these applications varies in all three space dimensions, e.g., velocity varies along a channel, across the channel, and from the water surface to the channel bottom. However, normally the spatial variation in the velocity across the channel and as a function of depth is negligible, so that the entire flow process can be approximated as varying in only one space dimension -- the x-direction along the flow channel. Thus, the **one-dimensional** equations of unsteady flow are widely applicable.

Simplified Distributed Routing Models. Prior to the advent of computers, or more recently the feasible economical availability of such computational resources, the inability to obtain any solutions at all to the complete Saint-Venant equations resulted in the development of several simplified distributed routing models. They are based on the mass conservation equation (10.3.1) and various simplifications of the momentum equation (10.3.2).

Kinematic wave model. The most simple type of distributed routing model is the **kinematic wave model**, interest in which was stimulated by the work of Lighthill and Whitham (90). It is based on the following simplified form of the momentum equation:

$$S_f - S_o = 0 \qquad (10.3.3)$$

in which S_o is the bottom slope of the channel (watercourse) and a component of the term $(\partial h/\partial x)$. This assumes that the momentum of the unsteady flow is the same as that of steady, uniform flow described by the Chezy, Manning equation or a similar expression in which discharge is a single-valued function of depth, i.e., $\partial A/\partial Q = dA/dQ = 1/c$. Also, since $\partial A/\partial t = \partial A/\partial Q \cdot \partial Q/\partial t$ and $Q = AV$, (10.3.1) can

be expanded into the classical **kinematic wave equation**, i.e.,

$$\frac{\partial Q}{\partial t} + c \frac{\partial Q}{\partial x} - cq = 0 \qquad (10.3.4)$$

in which the **kinematic wave velocity** or **celerity** (c) is defined as:

$$c = k'V \qquad (10.3.5)$$

where k' is the **kinematic ratio**, i.e., the kinematic wave celerity divided by the flow velocity (V). If the Manning equation is used for the steady uniform flow, the kinematic ratio is given by the following expression:

$$k' = 1/V \; dQ/dA = 5/3 - 2/3 \; A/(BP) \; dP/dy \qquad (10.3.6)$$

in which B is the wetted top width, A the wetted area, P the perimeter of the wetted portion of the cross section, and dP/dy is the derivative of P with respect to the water depth (y). For flow in a wide, rectangular channel, k' = 5/3. Solution methods for the kinematic wave equation (10.3.4) can consist of an analytical solution using the method of characteristics (19,90,127) or direct solution by finite-difference approximation techniques of either explicit or implicit types (19,28,59,65,86,91,124). The kinematic wave equation does not theoretically account for hydrograph (wave) attenuation. It is only through the numerical error associated with the finite-difference solution that attenuation is achieved. Kinematic wave models are limited to applications where single-value, stage-discharge ratings exist -- where there are no **loop-ratings** --and where backwater effects are insignificant. Since, in kinematic wave models, flow disturbances can propagate only in the downstream direction, **reverse (negative) flows** cannot be predicted. Kinematic wave models are appropriately used as components of hydrologic watershed models (28,59) for overland flow routing of runoff; they are not recommended for channel routing unless the hydrograph is very slow rising, the channel slope is moderate to steep, and hydrograph attenuation is quite small. See Section 10.1.2 for the kinematic wave model's relative accuracy properties.

Diffusion wave model. Another simplified distributed routing model, known as the **diffusion wave (zero-inertia) model**, is based on (10.3.1) along with an approximation of the momentum equation that retains only the last two terms in (10.3.2), i.e.,

$$\partial h/\partial x + S_f = 0 \qquad (10.3.7)$$

Finite-difference approximation techniques, both explicit (58) and implicit (131), have been used to obtain simultaneous solutions to (10.3.1) and (10.3.7). This type of simplified routing model considers backwater effects but improperly distributes them instantaneously (in time) throughout the total routing reach; its accuracy is also deficient for very fast rising hydrographs, such as those resulting from dam failures, hurricane storm surges, or rapid reservoir releases, which propagate through mild to flat sloping watercourses. See Section 10.1.2 for the diffusion model's relative accuracy properties. Several types of distributed

flow routing models (dynamic, diffusion, and kinematic) are listed in Table 10.3.1.

10.3.2 Muskingum-Cunge Method

The Muskingum method can be modified by computing the routing coefficients in a particular way as shown by Cunge (23) and others (32,77,94) which changes the kinematic-based Muskingum method to one based on the diffusion analogy which is capable of predicting hydrograph attenuation. This modified Muskingum method (known as the **Muskingum-Cunge method**) is most effectively used as a distributed flow routing technique (19,44,77,94,101,108,112). The recursive equation applicable to each Δx_i subreach for each Δt^j time step is:

$$Q_{i+1}^{j+1} = C_1 Q_i^{j+1} + C_2 Q_i^j + C_3 Q_{i+1}^j + C_4 \qquad (10.3.8$$

which is similar to the Muskingum method (10.2.7), but expanded to include lateral inflow effects, C_4. Q_i^{j+1} is the same as I_{j+1} in (10.2.7) while Q_i^j and Q_{i+1}^j are the same as I_j and Q_j, respectively. The coefficients C_1, C_2, and C_3 are positive values whose sum must equal unity; they are defined as in (10.2.8-10.2.10). The last term (C_4) in (10.3.8) accounts for the effect of time (Δt) and space (Δx) averaged lateral inflow ($\bar{q}_i$), i.e.,

$$C_4 = \bar{q}_i \, \Delta x \, \Delta t / [2K(1-X) + \Delta t] \qquad (10.3.9$$

in which K is a **storage constant** having dimensions of time, and X is a **weighting factor** expressing the relative importance inflow and outflow have on the storage. It can be shown (23,94) that (10.3.8) is a finite-difference representation of the classical kinematic wave equation (10.3.4); however, if X is expressed as a particular function of the flow properties, (10.3.8) can be considered an approximate solution of a combination of (10.2.1) and (10.3.7) known as the parabolic, diffusion analogy equation which accounts for wave attenuation but not for reverse (negative) flows or backwater effects. It's relative accuracy is approximately defined by (10.1.3). In the Muskingum-Cunge method, K and X are computed as follows:

$$K = \Delta x / \bar{c} \qquad (10.3.10$$

$$X = 0.5 \left[1 - \bar{Q} / (\bar{c} \, \bar{B} \, S_e \, \Delta x) \right] = 0.5 \left[1 - \bar{D} / (\bar{k}' \, S_e \, \Delta x) \right] \qquad (10.3.11$$

in which $\bar{c}$ is the kinematic wave celerity (10.3.5), $\bar{Q}$ is discharge, $\bar{B}$ is cross sectional topwidth associated with $\bar{Q}$, S_e is the energy slope approximated by evaluating S_f in (10.3.2) for the initial flow condition, $\bar{D}$ is the hydraulic depth (A/B), and $\bar{k}'$ is the kinematic wave ratio (10.3.6). The bar (-) indicates that variable is averaged over the Δx reach and over the Δt time step. For minimal numerical errors associated with the solution scheme, the time step (Δt) and distance step (Δx) should be selected as follows (73):

$$\Delta t \leq T_r/M \tag{10.3.12}$$

where $M \geq 5$, T_r is the time of rise of the hydrograph, and

$$\Delta x \simeq 0.5\ c\ \Delta t \left[1 + \left(1 + 1.5\ \bar{q}/(c^2\ S_o \Delta t)\right)^{1/2}\right] \tag{10.3.13}$$

in which $\bar{q}$ is the average unit-width discharge (Q/B) and S_o the bottom slope.

Solution Procedure. With coefficients defined by (10.2.8)-(10.2.10) and (10.3.9)-(10.3.11), the solution of (10.3.8) can be obtained by either linear or nonlinear (iterative) methods (101,108,112). The coefficients are functions of Δx and Δt (the independent parameters) and D, c, and k' (the dependent variables) are also functions of water-surface elevations (h). These may be obtained from a steady, uniform flow formula such as the **Manning equation** (17,18,19,61,91,96), i.e.,

$$Q = \mu/n\ AR^{2/3}\ S_e^{1/2} \tag{10.3.14}$$

in which n is the **Manning roughness coefficient**, A is the cross-sectional area, R is the hydraulic radius given by A/P in which P is the wetted perimeter of the cross section, S_e is the energy slope computed via a backwater equation (see Initial Conditions in Section 10.3.3) for only the initial flow to properly approximate S_e for channels with irregular and even adverse bottom slopes, and μ is a units conversion (17) factor (1.49 for US and 1.0 for SI).

In the **linear solution** procedure, the coefficients K and X are assumed constant for all time steps in each reach, or they are computed from the known flow properties, i.e., Q(i,j), Q(i,j+1), Q(i+1,j), h(i,j), h(i,j+1), and h(i+1,j). In the more accurate **nonlinear solution**, an estimated value of the unknown flow (Q_{i+1}^{j+1}) and its corresponding h value is also used to compute K and X. The estimated values are determined by extrapolation from previously computed values. The solution procedure is iterative and converges when computed and estimated values of h agree within a suitably small tolerance, say 0.01 ft (0.003 m).

Limitations. The nonlinear Muskingum-Cunge routing method is limited to hydrographs that are not fast rising such as those produced by dam failures (errors exceed 5 percent when $T_r \geq 0.002/S_o^{1.1}$); also, backwater effects and reverse flows are not accounted for in this method.

10.3.3 Dynamic Routing

General. If the complete Saint-Venant equations (10.3.1) and (10.3.2) are used, the routing model is known as a **dynamic routing model**. With the advent of high-speed computers, Stoker (126,127) first attempted in 1953 to use the complete Saint-Venant equations for routing Ohio River floods (69). Since then, much effort has been expended on the development of dynamic routing models. Many models have been reported in the literature (44,88,95), some of which are listed in Table 10.3.1.

Classification of dynamic routing methods. Dynamic routing models can be categorized as characteristic and direct methods of solving the Saint-Venant equations. In the **characteristic methods**, these equations are first transformed into an equivalent set of four ordinary differential equations which are then approximated with finite differences to obtain solutions. Characteristic methods (1,6,10,61,83,88,128) have not proven advantageous over the direct methods for practical flow routing applications.

Direct methods can be classified further as either explicit or implicit. **Explicit schemes** (9,33,54,69,71,88,89,126,130,139) transform the differential equations into a set of algebraic equations which are solved sequentially for the unknown flow properties at each cross section at a given time. However, **implicit schemes** (4,7,10,11,19,25,26,33,35,37,38,40,41,44,45,49,63,72,75,80,88,91,109,114,119, 120,130,137,138) transform the Saint-Venant equations into a set of algebraic equations which must be solved simultaneously for all Δx computational reaches at a given time; this set of simultaneous equations may be either linear or nonlinear, the latter requiring an iterative solution procedure.

Numerical stability of solution. Explicit methods, although simpler in application, are restricted by **numerical stability** considerations. Stability problems arise when inevitable errors in computational round-off and those introduced in approximating the partial differential equations via finite differences accumulate to the point that they destroy the usefulness and integrity of the solution, if not the total breakdown of the computations, by creating artificial oscillations of length about $2\Delta x$ in the solution. Due to stability requirements, explicit methods require very small computational time steps on the order of a few seconds or minutes depending on the ratio of the computational reach length (Δx) to the minimum dynamic wave celerity (u), i.e., $\Delta t \leq \Delta x/u$. This is known as the **Courant condition**, and it restricts the time step to less than that required for an infinitesimal disturbance to travel the Δx distance. Such small time steps cause explicit methods to be very inefficient in the use of computer time.

Implicit finite-difference techniques, however, have no restrictions on the size of the time step due to mathematical stability; however, **numerical convergence** (accuracy) considerations require some limitation in time step size. Implicit techniques are generally preferred over explicit because of their computational efficiency. Rather than using finite-difference approximation techniques to solve the Saint-Venant equations, finite element techniques (22,29,56) can be used; however, their greater complexity offsets any apparent advantages when compared to a weighted, four-point implicit finite-difference scheme (described later) for solving the one-dimensional flow equations. Finite element techniques are often applied to two- and three-dimensional flow computation.

Extended Saint-Venant Equations. More powerful and useful expressions of the Saint-Venant equations are their **conservation** or **divergent** form with additional terms to account for lateral flows (87,127,129), off-channel storage areas (33,87,129), and sinuosity effects (29,30). The **extended Saint-Venant equations** (45) consist of the mass conservation equation, i.e.,

$$\partial Q/\partial x + \partial s_c(A + A_o)/\partial t - q = 0 \qquad (10.3.15)$$

and the momentum equation, i.e.,

$$\partial(s_m Q)/\partial t + \partial(\beta Q^2/A)/\partial x + gA(\partial h/\partial x + S_f + S_{ec}) + L + W_f B = 0 \quad (10.3.16)$$

where h is the water-surface elevation, A is the active cross-sectional area of flow, A_o is the inactive (**off-channel storage**) cross-sectional area which may be preferred omitted (25) and its effect represented by a higher frictional resistance for that portion of the cross-section, s_c and s_m are depth-weighted **sinuosity coefficients** (29,30,45) which correct for the departure of a sinuous in-bank channel from the x-axis of the floodplain, x is the longitudinal mean flow-path distance measured along the center of the watercourse (channel and floodplain), t is time, q is the lateral inflow or outflow per lineal distance along the watercourse (inflow is positive and outflow is negative), β is the **momentum coefficient** for nonuniform velocity distribution within the cross section (87,130), g is the gravity acceleration constant, S_f is the boundary friction slope, and S_{ec} is the expansion-contraction (large eddy loss) slope (45,114).

Friction slope. The boundary friction slope (S_f) is evaluated from Manning's equation for uniform, steady flow, i.e.,

$$S_f = n^2|Q|Q/(\mu^2 A^2 R^{4/3}) = |Q|Q/K_c^2 \quad (10.3.17)$$

in which n is the Manning coefficient of frictional resistance, R is the hydraulic radius, μ is a units conversion factor (1.49 for US units and 1.0 for SI), and K_c is the **channel conveyance** factor. The absolute value of Q is used to correctly account for reverse (negative) flows. The conveyance formulation is preferred (for numerical and accuracy considerations) for composite channels (25,45) having wide, flat overbanks or floodplains in which K_c represents the sum of the conveyance of the channel (which is corrected for sinuosity effects by dividing by s_m), and the conveyances of left and right overbank areas.

Expansion/contraction effects. The term (S_{ec}) is computed as follows:

$$S_{ec} = K_{ec}\Delta(Q/A)^2/(2g\ \Delta x) \quad (10.3.18)$$

in which K_{ec} is the **expansion/contraction coefficient** (negative for contraction, positive for expansion) which varies from -0.8 to 0.4 for an abrupt change in section geometry to -0.3 to 0.1 for a very gradual, warped transition between cross sections. The Δ represents the difference in the term $(Q/A)^2$ at two adjacent cross sections separated by a distance Δx. If the flow direction changes from downstream to upstream, K_{ec} can be automatically changed (45).

Routing parameters. The depth-weighted sinuosity coefficients are depth dependent and computed from specified **sinuosity factors** which are ≥ 1; they represent the ratio of the flow-path distance along a meandering channel to the mean flow-path distance along the floodplain.

The momentum correction coefficient (β) for nonuniform velocity distribution is:

$$\beta = \frac{K_{c_\ell}^2/A_\ell + K_{c_c}^2/A_c + K_{c_r}^2/A_r}{\left(K_{c_\ell} + K_{c_c} + K_{c_r}\right)^2/\left(A_\ell + A_c + A_r\right)} \qquad (10.3.19)$$

in which K_c is conveyance, A is wetted area, and the subscripts ℓ, c, and r denote left floodplain, channel, and right floodplain, respectively (17,45). When floodplain properties are not separately specified and the total cross section is treated as a composite section, β can be approximated as $1.0 \leq \beta \leq 1.06$.

Lateral flow momentum. The term (L) in (10.3.16) is the momentum effect of lateral flows, and has the following form (130): (a) lateral inflow, $L = -qv_x$, where v_x is the velocity of lateral inflow in the x-direction of the main channel flow; (b) seepage lateral outflow, $L = -0.5qQ/A$; and (c) bulk lateral outflow, $L = -qQ/A$.

Wind effects. The last term ($W_f B$) in (10.3.16) represents the resistance effect of wind on the water surface (39,87); B is the wetted topwidth of the active flow portion of the cross section; and $W_f = V_r|V_r|\, c_w$, where the wind velocity relative to the water is $V_r = V_w \cos w - V$, V_w is the velocity of the wind, w is the acute angle the wind direction makes with the x-axis, V is the velocity of the unsteady flow, and c_w is a wind friction coefficient (33).

Mud or debris flows. Another term (S_i) can be included in the momentum equation (10.3.16) in addition to S_f to account for viscous dissipation of **non-Newtonian flows** such as mud or debris flows (45). This effect becomes significant (103) only when the solids concentration of the flow is in the range of about 40 to 50 percent by volume. For concentrations of solids greater than about 50 percent, the flow behaves more as a landslide and is not governed by the Saint-Venant equations.

Implicit Four-Point, Finite-Difference Solution Technique. The extended Saint-Venant equations (10.3.15) and (10.3.16) constitute a system of partial differential equations with two independent variables, x and t, and two dependent variables, h and Q; the remaining terms are either functions of x, t, h, and/or Q, or they are constants. The partial differential equations can be solved numerically by approximating them with a set of finite-difference algebraic equations; then the system of algebraic equations are solved in conformance with prescribed initial and boundary conditions.

Of various implicit, finite-difference solution schemes that have been developed, a **weighted four-point scheme** first used in 1961 by Preissmann (109) and more recently by many others (4,7,11,15,19,25,26,35,37,38,39,40,41,44,45,49,63,72,80, 91,119,120,137,138) is most advantageous. It is readily used with unequal distance steps and its stability-convergence properties are conveniently modified, and boundary conditions are easily applied.

The space-time plane. In the weighted four-point implicit scheme, the continuous x-t region in which solutions of h and Q are sought is represented by a rectangular grid of discrete points as shown in Fig. 10.3.1. The **x-t plane**

(solution domain) is a convenient device for visualizing relationships among the variables. The grid points are determined by the intersection of lines drawn parallel to the x- and t-axes. Those parallel to the t-axis represent locations of cross sections; they have a spacing of Δx, which need not be the same between each pair of cross-sections. Those parallel to the x-axis represent time lines; they have a spacing of Δt, which also need not be the same between successive time points. Each point in the rectangular network can be identified by a subscript (i) which designates the x-position or cross section and a superscript (j) which designates the particular time line.

Numerical approximations of derivatives. The time derivatives are approximated by a forward-difference quotient at point M (in Fig. 10.3.1) centered between the i and i+1 points along the x-axis, i.e.,

$$\partial\phi/\partial t \simeq (\phi_i^{j+1} + \phi_{i+1}^{j+1} - \phi_i^j - \phi_{i+1}^j) / (2\ \Delta t_j) \qquad (10.3.20)$$

where ϕ represents any dependent variable or functional quantity (Q, s_c, s_m, A, A_o, q, h). Spatial derivatives are approximated at point M by a forward-difference quotient located between two adjacent time lines according to weighting factors of θ (the ratio $\Delta t'/\Delta t$ shown in Fig. 10.3.1) and $1-\theta$, i.e.,

$$\partial\phi/\partial x \simeq \theta(\phi_{i+1}^{j+1} - \phi_i^{j+1}) / \Delta x_i + (1-\theta)(\phi_{i+1}^j - \phi_i^j) / \Delta x_i \qquad (10.3.21)$$

Non-derivative terms are approximated with weighting factors at the same time level (point M) where the spatial derivatives are evaluated, i.e.,

$$\phi \simeq \theta(\phi_i^{j+1} + \phi_{i+1}^{j+1}) / 2 + (1-\theta)(\phi_i^j + \phi_{i+1}^j) / 2 \qquad (10.3.22)$$

Stability of the implicit scheme. The weighted four-point implicit scheme is unconditionally, linearly stable for $\theta \geq 0.5$; however, the sizes of the Δt and Δx steps are limited by the accuracy of the assumed linear variations of functions between the grid points in the x-t solution domain. Values of θ greater than 0.5 dampen parasitic oscillations which have wave lengths of about $2\Delta x$ that can grow enough to invalidate or destroy the solution. The θ weighting factor causes some loss of accuracy as it departs from 0.5, a **box scheme** (7,69), and approaches 1.0, a **fully implicit scheme** (10). This effect becomes more pronounced as the magnitude of the Δt step increases (38). Usually, a θ weighting factor of 0.60 is used to minimize the loss of accuracy while avoiding the possibility of weak (pseudo) instability for θ values of 0.5 when frictional effects are minimal (2,38,88).

Algebraic routing equations. Using the finite-difference operators of (10.3.20) - (10.3.22) to replace the derivatives and other variables in (10.3.15) and (10.3.16), the following weighted four-point, **implicit finite-difference equations** are obtained:

$$\theta\left[\frac{Q_{i+1}^{j+1} - Q_i^{j+1}}{\Delta x_i}\right] - \theta\, q_i^{j+1} + (1-\theta)\left[\frac{Q_{i+1}^{j} - Q_i^{j}}{\Delta x_i}\right] - (1-\theta)\, q_i^{j} +$$

$$\left[\frac{s_{c_i}^{j+1}(A+A_o)_i^{j+1} + s_{c_i}^{j+1}(A+A_o)_{i+1}^{j+1} - s_{c_i}^{j}(A+A_o)_i^{j} - s_{c_i}^{j}(A+A_o)_{i+1}^{j}}{2\Delta t_j}\right] = 0 \qquad (10.3.2$$

$$\left[\frac{\left(s_{m_i}Q_i\right)^{j+1} + \left(s_{m_i}Q_{i+1}\right)^{j+1} - \left(s_{m_i}Q_i\right)^{j} - \left(s_{m_i}Q_{i+1}\right)^{j}}{2\Delta t_j}\right] + \theta\left[\frac{(\beta Q^2/A)_{i+1}^{j+1} - (\beta Q^2/A)_i^{j+1}}{\Delta x_i}\right.$$

$$\left. + g\,\bar{A}_i^{j+1}\left(\frac{h_{i+1}^{j+1} - h_i^{j+1}}{\Delta x_i} + \bar{S}_{f_i}^{j+1} + S_{ec_i}^{j+1}\right) + L_i^{j+1} + (W_f\bar{B})_i^{j+1}\right] + (1-\theta)$$

$$\left[\frac{(\beta Q^2/A)_{i+1}^{j} - (\beta Q^2/A)_i^{j}}{\Delta x_i} + g\,\bar{A}_i^{j}\left(\frac{h_{i+1}^{j} - h_i^{j}}{\Delta x_i} + \bar{S}_{f_i}^{j} + S_{ec_i}^{j}\right) + L_i^{j} + (W_f\bar{B})_i^{j}\right] = 0 \qquad (10.3.2$$

where:

$$\bar{A}_i = (A_i + A_{i+1})/2 \qquad (10.3.25)$$

$$\bar{S}_{f_i} = n^2\,\bar{Q}_i\left|\bar{Q}_i\right|/(\mu^2\,\bar{A}_i^2\,\bar{R}_i^{4/3}) = \bar{Q}\left|\bar{Q}\right|/\bar{K}_{c_i}^2 \qquad (10.3.26)$$

$$\bar{Q}_i = (Q_i + Q_{i+1})/2 \qquad (10.3.27)$$

$$\bar{R}_i = \bar{A}/\bar{P} \simeq \bar{A}/\bar{B} \qquad (10.3.28)$$

$$\bar{B}_i = (B_i + B_{i+1})/2 \qquad (10.3.29)$$

$$\bar{K}_{c_i} = (K_{c_i} + K_{c_{i+1}})/2 \qquad (10.3.30)$$

The terms L and W_fB are defined in (10.3.16); terms associated with the j^{th} time line are known from initial conditions or previous time-step computations; and μ in (10.3.26) is defined in (10.3.17).

Solution Procedure. The flow equations are expressed in finite-difference form for all Δx reaches between the first and last (N-th) cross section (i = 1,2,...,N) along the watercourse and then solved simultaneously for the unknowns (Q and h)

at each cross section. In essence, the solution technique determines the unknown quantities (Q and h at all specified cross sections along the watercourse) at various times into the future; the solution is advanced from one time to a future time over a finite time interval **(time step)** of magnitude Δt. Thus, applying (10.3.23) and (10.3.24) recursively to each of the (N-1) rectangular grids in Fig. 10.3.1 between the upstream and downstream boundaries, a total of (2N-2) equations with 2N unknowns are formulated. Then, prescribed **boundary conditions** for **subcritical flow** (**Froude number** less than unity, i.e., $Fr = V/\sqrt{gD} < 1$), one at the upstream boundary and one at the downstream boundary, provide the two additional and necessary equations required for the system to be determinate. Since disturbances can propagate only in the downstream direction in **supercritical flow** ($Fr > 1$), two upstream boundary conditions are required for the system to be determinate. The boundary conditions are described later. Due to the nonlinearity of (10.3.23) and (10.3.24) with respect to Q and h, an iterative, highly efficient quadratic solution technique, such as the **Newton-Raphson method** (7,19,44,45,68) is frequently used. Other solution techniques linearize (10.3.23) and (10.3.24) via a Taylor series expansion (11,25,26,109,120) or other means (130). Convergence of the iterative technique is attained when the difference between successive solutions for each unknown is less than a relatively small prescribed tolerance. Convergence for each unknown at all cross sections is usually attained within about one to five iterations. A more complete description of the solution method may be found elsewhere (7,19,25,39,44,91).

The solution of 2N x 2N simultaneous equations requires an efficient technique for the implicit method to be feasible. One such procedure requiring 38N computational operations (+, -, *, /) is a **compact, penta-diagonal Gaussian elimination method** (36,39,44) which makes use of the banded structure of the coefficient matrix of the system of equations. This is essentially the same as the **double sweep** elimination method (2,25,33,72,88,110).

When flow is supercritical, the solution technique previously described can be somewhat simplified. Two boundary conditions are required at the upstream boundary (2,40) and none at the downstream boundary since flow disturbances cannot propagate upstream in supercritical flow. The unknown h and Q at the most upstream cross section are determined from the two boundary equations. Then, cascading from upstream to downstream, (10.3.23) and (10.3.24) are solved for h_{i+1} and Q_{i+1} at each cross section by using Newton-Raphson iteration applied to a system of two nonlinear equations with two unknowns.

Initial Conditions. Values of water-surface elevation (h) and discharge (Q) for each cross section must be specified initially at time t = 0 to obtain solutions to the Saint-Venant equations. **Initial conditions** may be obtained from any of the following: (a) observations at gaging stations, or interpolated values between gaging stations for intermediate cross sections in large rivers; (b) computed values from a previous unsteady flow solution (used in real-time flood forecasting); and (c) computed values from a steady-flow backwater solution. The backwater method is most commonly used, in which the steady discharge at each cross section is determined by:

$$Q_{i+1} = Q_i + q_i \Delta x_i \qquad \ldots\ i = 1,2,3,\ldots,N-1 \qquad (10.3.31)$$

in which Q_1 is the assumed steady flow at the upstream boundary at time t=0, and q_i is the known average lateral inflow or outflow along each Δx reach at t=0. The water-surface elevations (h_i) are computed according to the following steady-flow simplification of the momentum equation (10.3.24):

$$(Q^2/A)_{i+1} - (Q^2/A)_i + g\bar{A}_i\,(h_{i+1} - h_i + \Delta x_i\,\bar{S}_{f_i}) = 0 \qquad (10.3.32$$

in which $\bar{A}_i$ and $\bar{S}_{f_i}$ are defined by (10.3.25) and (10.3.26), respectively. The computations proceed in the upstream direction (i = N-1, ... 3,2,1) for subcritical flow (they must proceed in the downstream direction for supercritical flow). The starting water-surface elevation (h_N) can be specified or obtained from the appropriate downstream boundary condition for the discharge (Q_N) obtained via (10.3.30). The Newton-Raphson iterative solution method (48,68) for a single equation and/or a simple, less efficient, but more stable bi-section iterative technique can be applied to (10.3.32) to obtain h_i. The steady water-surface profile can also be obtained from steady-flow backwater models such as HEC-2 (66), WSP2 (125), or WSPRO (121). The initial conditions must be sufficiently accurate to result in convergence of the Newton-Raphson solution of the Saint-Venant finite-difference equations. Small initial errors will dampen out after several time steps due to friction.

External Boundaries. Values for the unknowns at **external boundaries** (the upstream and downstream extremeties of the routing reach) of the watercourse, must be specified in order to obtain solutions to the Saint-Venant equations. In fact, in most unsteady flow applications, the unsteady disturbance is introduced at one or both of the external boundaries.

Upstream boundary. Either a specified discharge or water-surface elevation **time series** (**hydrograph**) can be used as the **upstream boundary condition**. The hydrograph should not be affected by downstream flow conditions.

Downstream boundary. Specified discharge or water-surface elevation time series, or a tabular relation between discharge and water-surface elevation (single-valued rating curve) can be used as the **downstream boundary condition**.

Another downstream boundary condition can be a **loop-rating curve** based on the Manning equation (39,40,44,45). The loop is produced by using the friction slope (S_f) rather than the channel bottom slope (S_o). The friction slope exceeds the bottom slope during the rising limb of the hydrograph while the reverse is true for the recession limb. The friction slope (S_f) is approximated by using (10.3.16) where L and W_f are assumed to be zero while s_m and ß are assumed to be unity, i.e.,

$$S_f \simeq -\left(Q_N^j - Q_N^{j-1}\right)/\left(gA_n^j\,\Delta t^j\right) - \left[\left(Q^2/A\right)_N^j - \left(Q^2/A\right)_{N-1}^j\right]/ \left(gA_N^j\,\Delta x_{N-1}\right) - \left(h_N^j - h_{N-1}^j\right)/\Delta X_{N-1} \qquad (10.3.33$$

The loop-rating boundary equation allows the unsteady wave to pass the downstream boundary with minimal disturbance by the boundary itself, which is desirable wher

the routing is terminated at an arbitrary location along the watercourse and not at a location of actual flow control such as a dam.

The downstream boundary condition can also be a **critical flow** section such as the entrance to a waterfall or a steep reach, i.e.,

$$Q = \sqrt{g/B}\ A^{3/2} \tag{10.3.34}$$

Critical flow occurs when the bottom slope (S_o) exceeds the **critical slope** (S_c) which can be easily computed as follows:

$$S_c = \hat{\mu}\ n^2/D^{1/3} \tag{10.3.35}$$

where $\hat{\mu}$ = 14.6 for US units and $\hat{\mu}$ = 9.8 for SI units.

When the downstream boundary is a stage/discharge relation (rating curve), the flow at the boundary should not be otherwise affected by flow conditions further downstream. Although there are often some minor effects due to the presence of cross-sectional irregularities downstream of the chosen boundary location, these usually can be neglected unless the irregularity is so pronounced as to cause significant backwater or drawdown effects. Reservoirs or major tributaries located below the downstream boundary which cause backwater effects at the boundary should be avoided. When either of these situations are unavoidable, the routing reach should be extended downstream to the dam in the case of the reservoir or to a location downstream of where the major tributary enters. Sometimes the routing reach may be shortened by moving the downstream boundary to a location further upstream where backwater effects are negligible.

Internal Boundaries. Along a watercourse, there are locations such as a dam, bridge, or waterfall (short rapids) where the flow is rapidly varied rather than gradually varied in space. At such locations (**internal boundaries**), the Saint-Venant equations are not applicable since gradually varied flow is a necessary condition for their derivation. Empirical water elevation-discharge relations such as weir-flow are utilized for simulating rapidly varying flow. At internal boundaries, cross sections are specified for the upstream and downstream extremities of the section of watercourse where rapidly varying flow occurs. The Δx reach containing an internal boundary requires two internal boundary equations; since, as with any other Δx reach, two equations equivalent to the Saint-Venant equations are required. One of the required internal boundary equations represents conservation of mass with negligible time-dependent storage, i.e.,

$$Q_i - Q_{i+1} = 0 \tag{10.3.36}$$

The second equation is usually an empirical **rapidly-varied flow** relation of the type, $Q = f(h_i, h_{i+1})$. Several examples of rapidly-varied flow internal boundary equations are listed in Table 10.3.2.

Selection of Computational Δx and Δt. The accuracy of the finite-difference solution is affected by the choice of the computational distance step (Δx). For best accuracy, the maximum computational distance step (Δx_m) is selected as follows (44,45,111,141):

$$\Delta x_m \leq c\ T_r/20 \qquad (10.3.37)$$

in which c is the **bulk wave celerity** (the celerity associated with an essential characteristic of the unsteady flow such as the peak of the hydrograph). In most applications, the wave speed is well approximated as a kinematic wave, and c is estimated from (10.3.5) or from two or more observed flow hydrographs at different points along the channel. Since c can vary along the channel, Δx_m may not be constant along the channel.

Another criterion for selecting Δx_m is the restriction imposed by rapidly varying cross-sectional changes along the x-axis of the watercourse. Such expansion/contraction is limited to the following inequality (13,117):

$$0.635 < A_{i+1}/A_i < 1.576 \qquad (10.3.38)$$

This condition results in the following approximation for the maximum computational distance step (45):

$$\Delta x_m < L'/\left[1+ 2\left|A_i - A_{i+1}\right|/\hat{A}\right] \qquad (10.3.39)$$

where $\hat{A} = A_{i+1}$ for a contracting reach and $\hat{A} = A_i$ for an expanding reach, and L' is the original distance step between adjacent specified cross sections at i and i+1. The selection of Δx is determined by the minimum value of Δx_m from either (10.3.37) or (10.3.39).

Significant changes in the bottom slope of the watercourse also require small distance steps in the vicinity of the change. This is required particularly when the flow changes from subcritical to supercritical or conversely along the watercourse. Such changes can require computational distance steps in the range of 50 to 200 ft (15 to 61 m).

Selection of the Δt time step is governed by the following inequality:

$$\Delta t \leq T_r/M \qquad (10.3.40)$$

where M is a numerical accuracy factor varying between 5 and 30; M can be estimated as $2.67\left[1 + \sqrt{g}\ n/(\mu D^{1/6} S_o^{1/2})\right]$ to provide desirable numerical error properties; μ is defined in (10.3.17); and T_r is the smallest time of rise of any wave that is routed.

10.4 DATA REQUIREMENTS FOR ROUTING MODELS

10.4.1 General

The data required for routing models are substantially different for the lumped models than for the distributed models. An inflow (discharge) hydrograph is always required for lumped models. Also, this is required for distributed models, although the diffusion (zero-inertia) and dynamic models can use a water-surface

elevation time series as an alternate upstream boundary condition. The different data requirements for lumped and distributed models are shown in Table 10.4.1. The remaining portion of this subsection will provide additional information on cross-sectional, channel friction (Manning n), and lateral flow data.

10.4.2 Cross Sections

Much of the uniqueness of a specific distributed flow routing application is captured in the **cross sections** located at selected points along the water course as in Fig. 10.1.1.

Active Sections. That portion of the channel cross section in which flow occurs is called **active.** Cross sections may be of regular or irregular geometrical shape. As indicated in Fig. 10.4.1, each cross section is described by tabular values of channel topwidth and water-surface elevation which constitute a piece-wise linear relationship. Generally about 4 to 12 sets of topwidths and associated elevations provide a sufficiently accurate description of the cross section. Area-elevation tables can be generated initially from the specified topwidth-elevation data. Areas or widths associated with a particular water-surface elevation are linearly interpolated from the tabular values. Cross sections at gaging station locations are generally used as computational points. Such points are also specified at locations along the river where significant cross-sectional or flow-resistance changes occur or at locations where major tributaries enter. The spacing of cross sections can range from a few hundred feet to a few miles apart. Typically, cross sections are spaced farther apart for large rivers than for small streams, since the degree of variation in the cross-sectional characteristics is greater for the small streams. It is essential that the selected cross sections, with the assumption of linear variation between adjacent sections, represent the volume available to contain the flow along the watercourse. In some applications, particularly the routing of flood waves in large rivers with gradually varying cross sections, the number of required cross sections can be reduced by using a distance-weighted average section whose width is so computed that it replaces several (varying from a few to more than 50) intervening cross sections and yet conserves the volume within the reach (39,44).

Inactive (Dead) Sections. There can be portions of a cross section where the flow velocity in the x-direction is negligible relative to the velocity in the active portion. The inactive portion is called **off-channel (dead) storage;** it is represented by the term (A_o) in (10.3.15). Off-channel storage areas can be used to effectively account for adjacent embayments, ravines, or tributaries (see Fig. 10.4.1) which connect at some elevation with the flow channel but do not convey flow in the x-direction; they serve only to store some of the passing flow. Sometimes, off-channel storage can be used to simulate a heavily wooded floodplain which primarily stores some of the flood waters while conveying a very minimal portion of the flow. Dead storage cross-sectional properties are described by width (dead storage) vs. elevation tables.

10.4.3 Channel Friction

The resistance to flow (17,18,19,61,91,96,139) in a watercourse may be parameterized by the **Manning n, Chezy C, Darcy f,** or some other friction (roughness) coefficient which represents the effect of roughness elements of the channel bank and bed particles as well as form losses attributed to dynamic alluvial bed-forms

and vegetation of various types (grass, shrubs, field crops, brush, and trees) located along the banks and overbanks (floodplain). Also, small eddy losses due to mild expansion/contraction of cross-sectional reaches as well as river bend losses are often included as components of the Manning n (17).

The Manning n varies with the magnitude of flow (46). As the flow increases and more portions of the bank and overbank become inundated, the vegetation located at these elevations causes an increase in the resistance to flow (79). Also, the n value may be larger for small floodplain depths than for larger depths due to flattening of the brush, thick weeds, or tall grass as the flow depths and velocities increase. This effect may be reversed in the case of wooded overbanks where, at the greater depths, the flow impinges against the leaved branches rather than only against the tree trunks, thus increasing Manning's n. The n values may also decrease with increasing discharge when the increase in the overbank flow area is relatively small compared to the increase of flow area within the banks, as the case of wide rivers with levees situated closely along the natural river banks, or when floods remain confined within the channel banks.

Other conditions which can result in different n values for the same flow are: (a) change of season which affects the extent of vegetation, (b) change of water temperature which affects bed-forms in some alluvial rivers (20,135), (c) ice cover effects (17,102,136), and (d) man-made channel changes such as drift removal, channel straightening, bank stabilization, or paving.

The Manning n is defined for each channel reach and specified as a tabular piece-wise linear function of stage or discharge, with linear interpolation used to obtain n values intermediate to the tabulated values.

Calibration. Results from dynamic routing or other distributed routing models are somewhat sensitive to the Manning n. Best results are obtained when n is adjusted to reproduce historical observations of stage and discharge. Such an adjustment process is known as **calibration** which may be accomplished via either a trial-and-error or an automatic technique (44,51,141). In the absence of observed flows and water-surface elevations, selection of the Manning n should reflect the influence of bank and bed materials, channel obstructions, irregularity of the river banks, and especially vegetation. Vegetation may cause the n values to vary considerably with flow as previously described. Some basic references for estimating n values are available (12,17,18,19,61,91). Some references also describe the effects of urbanization of the floodplain (8,60, 140), wooded floodplains (8), and steep rivers with cobble/boulder beds (70). Manning n values for flows less than bankfull are approximately 0.015 - 0.035 for large rivers (Mississippi, Ohio, Missouri, Illinois), 0.03 - 0.04 for moderate sized rivers and streams, 0.04 - 0.07 for mountain streams, and 0.04 - 0.25 for overbank flows. Some references provide estimates of the Darcy friction factor (f) which is related to the Manning n as follows:

$$n = \tilde{\mu}\, f^{0.5}\, D^{0.17} \qquad (10.4.1)$$

where D is hydraulic depth, $\tilde{\mu}$ is 0.093 (US units) or 0.113 (SI units).

10.4.4 Lateral Flows

Specified unsteady flows associated with tributaries that are not dynamicall routed can be added to the unsteady flow along the routing reach. This i accomplished via the term q in (10.3.15) and (10.3.16). The total tributary flo which is a known function of time, i.e., Q(t) which is a specified time series is distributed along a single Δx reach, i.e., $q(t) = Q(t)/\Delta x_i$. Backwater effect of the routed flow on the tributary flow are ignored, and the **lateral flow** i usually assumed to enter perpendicular to the routed flow. Known outflows can b simulated by using a negative sign with the specified Q(t). Numerica difficulties in solving the Saint-Venant equations sometimes arise when the rati of lateral inflow to channel flow, q_i/Q_i, is too large; this can be overcome b increasing Δx_i for this reach.

10.5 FLOW ROUTING COMPLEXITIES

10.5.1 General

The routing of unsteady flows in natural waterways entails many complexities tha require special treatment. These include network of channels, levee overtopping mixed subcritical-supercritical flows, sediment transport effects, streamflow- aquifer interactions, ice effects, and two-dimensional flows.

10.5.2 Channel Networks

Flow routing is often required in natural waterways as well as man-made channel which are linked together forming a network of channels. The configuration ma be **dendritic** (tree-type) and/or **looped** (islands, parallel channels connected b bypasses, etc.). A network of channels presents complications in achievin computational efficiency when using implicit dynamic routing models. Necessar compatibility equations for flow conditions at the confluence of two channel produce a **coefficient matrix** in the solution procedure with elements which are no contained within the narrow band along the main-diagonal of the matrix. Such **off-diagonal elements** produce a **sparse matrix** containing relatively few nonzer elements. Unless special matrix solution techniques are used for the sparse matrix, the computational time required to solve the matrix by conventiona Gaussian elimination matrix solution techniques is too great and makes an implici solution infeasible. Various algorithms have been developed to provide efficient computational treatment of channel networks. Most algorithms treat the channe junctions as internal boundaries consisting of three compatibility equations, usually a conservation of mass equation and two simplified momentum equations (11,25,43,44,49,57,72). These are solved along with (10.3.23) and (10.3.24) applied to each Δx reach. The resulting sparse matrix is solved by various sparse matrix solution techniques of the **Gaussian elimination** or **double sweep** variety (25,36,43,44,57,72,75,88,120). Another type of network algorithm treats tributary flow at a junction as lateral flow (q) to the main-stem channel, and thereby eliminates the computational difficulty associated with off-diagonal elements; this is an iterative **relaxation** procedure (37,44) which is applicable only to first-order dendritic networks (a main-stem channel with one or more tributaries).

10.5.3 Supercritical/Subcritical Mixed Flow

Flow can change with either time or distance along the routing reach from supercritical to subcritical while passing through critical flow, or conversely. This **mixed flow** requires special treatment to prevent numerical instability when modeling it with the Saint-Venant equations. One method (43,44,45) of treating this is to avoid using the Saint-Venant equations at the point where mixed flow occurs; this is accomplished by dividing the routing reach at each time step into a series of subcritical and supercritical routing reaches (sub-reaches) and using appropriate external boundary conditions for each sub-reach. The Froude number is used to determine the supercritical reaches, for which Fr > 1. At each time step, the solution commences with the most upstream sub-reach, and proceeds sub-reach by sub-reach in the downstream direction. Hydraulic jumps are allowed to move at the end of a time step according to the relative values of supercritical sequent depth and the adjacent downstream subcritical depth. Another more approximate method that has been used for mixed flows is to arbitrarily decrease the ß coefficient in the second term of (10.3.16) so that it becomes zero as the flow approaches critical flow ($F_r = 1$). This rather crude approach helps to stabilize the numerical solution, but at the expense of accuracy since the second term $\partial(Q^2/A)/\partial x$ is thereby neglected in (10.3.16).

10.5.4 Levee Overtopping

Flows which overtop **levees** located along either or both sides of a main-stem river and/or its principal tributaries can be treated as lateral outflow (-q) in (10.3.15) and (10.3.16) where the diverted lateral flow over the levee is computed as broad-crested weir flow (25,43,44,45,49,138). This overtopping flow is corrected for submergence effects if the floodplain water-surface elevation sufficiently exceeds the levee crest elevation. The overtopping flow may reverse its direction when the floodplain elevation exceeds the river water-surface elevation, thus allowing flow to return to the channel after the flood peak passes. The overtopping broad-crested weir flow is computed according to the following:

$$q = -c_\ell K_s (h - h_c)^{3/2} \qquad (10.5.1)$$

where:

$$K_s = 1.0 \qquad \text{if } h_r \leq 0.67 \qquad (10.5.2)$$

$$K_s = 1.0 - 27.8 (\gamma - 0.67)^3 \qquad \text{if } h_r > 0.67 \qquad (10.5.3)$$

$$h_r = (h_{fp} - h_c) / (h - h_c) \qquad (10.5.4)$$

in which c_ℓ is the weir discharge coefficient ranging in value from 2.6 to 3.2 for US units (1.4 to 1.8 for SI units). K_s is the submergence correction factor (44,45) similar to that used for internal boundaries (dams), h_c is the levee-crest elevation, h is the water-surface elevation of the river, and h_{fp} is the water-surface elevation of the floodplain. Flow in the floodplain can affect the overtopping flows via the submergence correction factor, K_s. Flow may also pass

from the waterway to the floodplain through a time-dependent **crevasse** (**breach**) in the levee (11,41,49) via a breach-flow equation similar to that shown in Table 10.3.2. The floodplain, which is separated from the principal routing channel (river) by the levee, may be treated as: (a) a dead storage area (33,87,129) in the Saint-Venant equations; (b) a tributary which receives its inflow as lateral flow (the flow from the river which overtops the levee-crest) which is dynamically routed along the floodplain (41,44,49); and (c) flow and water-surface elevations can be computed by using a level-pool routing method (25,26,45,49,138) particularly if the floodplain is divided into compartments by levees or road embankments located perpendicular to the river levee.

10.5.5 Mobile-Bed Effects

A complex interaction of unsteady flow and sediment transport occurs in alluvial rivers with **mobile** (**moveable**) **sand beds** (15). The river bottom aggrades (raises) and degrades (lowers) during the passage of the flood wave. Also, the hydraulic resistance of the river bottom changes as the sand bed-forms change their magnitude and shape. Routing models which account for the effects of **aggradation** and **degradation** have been developed (15,16,63,67,72,80). In these models, the sediment conservation equation, i.e.,

$$(1 - \lambda)\ \partial A_b / \partial x + \partial Q_s / \partial x - q_s = 0 \qquad (10.5.5)$$

is coupled to an implicit finite-difference solution of the Saint-Venant equations. In (10.5.5) λ is the porosity of the bed material, A_b is the cross-sectional area of the mobile portion of the channel bed, Q_s is the volumetric sediment transport rate computed by some appropriate steady-flow sediment transport technique (5,34,93,134,142), and q_s is the lateral inflow rate of sediment per unit length. The coupling of (10.5.5) with (10.3.15) and (10.3.16) can be accomplished within the iteration of the nonlinear implicit solution, between these iterations, or simply between time steps of the flow computation; the particular type of coupling of water and sediment flow depends on the rate of change of A_b with respect to time. Also, the dynamic interaction between the changing sand bed-forms and bed friction may be approximated (14,132) via a continuous modification of the roughness coefficient (Manning n). Additional information on sediment transport is presented in Chapter 12.

10.5.6 Streamflow-Aquifer Interaction

Interaction of streamflow and its adjacent **groundwater aquifer** for floods occurring in some channels, particularly those often located in arid regions, can be of sufficient magnitude to affect the river flow by attenuating the peak flow, reducing the wave peak celerity, and extending the recession limb of the river discharge hydrograph. The flow between the river and the aquifer can be simulated by coupling distributed flow routing models to either one- or two-dimensional **groundwater models**. The coupling occurs through the lateral flow term (q) in the Saint-Venant equations. Both explicit (52) and implicit (106) dynamic flow routing models have been coupled to the unsteady saturated or saturated/unsaturated porous media equation. Time steps required for the flow routing equations are usually smaller than those required for the groundwater (saturated equations); models can take advantage of this for greater efficiency by solving the groundwater equations periodically.

10.5.7 Ice Effects

The formation of an ice cover in a waterway affects the flow (105). The ice cover floats except for those in narrow waterways or those with very thick covers located in extremely cold regions. The bottom of the ice cover causes an increase in the flow resistance coefficient (17). This varies over a wide range throughout the winter (102,136) as the ice cover begins to develop, reaches maturity, and then decays with increasing temperature. Localized hanging **ice-dams** further increase flow resistance. Severe increases in water-surface elevation can occur when **ice-jams** are formed during the break-up of the ice as air temperatures increase. The ice-jam can considerably reduce the cross-sectional area of flow and act as a constricted flow-control section. Ice effects can be considered in dynamic flow routing models (82,143). Ice effects are further discussed in Chapter 7.

10.5.8 Landslide-Generated Wave

Reservoirs are sometimes subject to landslides which move at high velocities into the reservoir; the slide displaces a portion of the reservoir contents and creates a very steep water wave which travels up and down the length of the reservoir (27), and the wave can overtop the dam and cause its failure (breach). A **landslide-generated wave** can be simulated by using a dynamic routing model. Using known information on the volume of landslide mass, its porosity, and the time interval over which the landslide moves into the reservoir, the landslide volume is deposited in the reservoir during very small time steps in the dynamic routing computations; this rapid reduction in reservoir cross-sectional area (45,78) creates a landslide-generated wave in the solution of the Saint-Venant equations. **Wave runup** for near vertical faces of concrete dams can be neglected; however, for earthen dams, the abrupt wave can advance up the sloping dam face to approximately 2.5 times the height of the wave (96).

10.5.9 Two-Dimensional Flows

Two-dimensional unsteady flow models which account for momentum conservation in the y-direction (across the waterway perpendicular to the x-axis) can be categorized as complete (all terms in the momentum equations are retained) or simplified (first two terms, inertial or acceleration terms in each momentum equation are neglected). Complete two-dimensional models (3,62,84,85) are used for unsteady flows in estuaries, bays, or lakes where environmental pollution concerns require knowledge of flow patterns (circulation) and velocities which are dominated by two-dimensional effects. Occasionally, simplified two-dimensional flow routing models have been used for unsteady flows in complex floodplains (24). Two-dimensional models are generally much more expensive to calibrate and execute on computers than one-dimensional models. Generally, the additional accuracy gained does not justify their use to predict water-surface elevations and average flows in typical unsteady flow applications having floodplains (138).

REFERENCES

1. Abbott, M.B. (1966). An Introduction to the Method of Characteristics, American Elsevier, New York.

2. Abbott, M.B. (1980). Computational Hydraulics, Pitman, London, England.

3. Abbott, M.B. and Cunge, J.A. (1975). 'Two-dimensional modeling of tidal deltas and estuaries,' Unsteady Flow in Open Channels, Vol. II, (Eds. K. Mahmood and V. Yevjevich), Chapter 18, pp. 763-812, Water Resources Pub. Fort Collins, Co.

4. Abbott, M.B. and Cunge, J.A. (1982). Engineering Applications of Computational Hydraulics, Vol. 1, Pitman, London, England.

5. Ackers, P. and White, W.R. (1973). 'Sediment transport: a new approach and analysis,' J. Hydraul. Div., ASCE, Vol. 99, No. HY11, pp. 2041-2060.

6. Amein, M. (1966). 'Streamflow routing on computer by characteristics,' Water Resources Res., Vol. 2, No. 1, pp. 123-130.

7. Amein, M. and Fang, C.S. (1970). 'Implicit flood routing in natural channels,' J. Hydraul. Div., ASCE, Vol. 96, No. HY12, pp. 2481-2500.

8. Arcement, G.J., Jr. and Schneider, V.R. (1984). Guide for Selecting Manning's Roughness Coefficients for Natural Channels and Flood Plains, Report No. RHWA-TS-84-204, U.S. Geological Survey for Federal Highway Administration, National Tech. Information Service, PB84-242585, 61 pp.

9. Balloffet, A. (1969). 'One-dimensional analysis of floods and tides in open channels,' J. Hydraul. Div., ASCE, Vol. 95, No. HY4, pp.1429-1451.

10. Baltzer, R.A. and Lai, C. (1968). 'Computer simulation of unsteady flow in waterways,' J. Hydraul. Div., ASCE, Vol. 94, No. HY4, pp. 1083-1117.

11. Barkow, R.L. (1990). UNET one-dimensional unsteady flow through a full network of open channels, Users Manual, Hydrologic Engineering Ctr., U.S. Army Corps of Engineers, Davis, Cal.

12. Barnes, H.H., Jr. (1967). Roughness Characteristics of Natural Channels, Geological Survey Water-Supply Paper 1849, United States Government Printing Office, Washington, D.C., 213 pp.

13. Basco, D.R. (1987). 'Improved robustness of the NWS DAMBRK algorithm,' Hydraulic Engineering, (Proc. of the 1987 National Conference on Hydraulic Engineering), ASCE, New York, Aug., pp. 776-781.

14. Brownlie, W.R. (1983). 'Flow depth in sand-bed channels,' J. Hydraul. Div., ASCE, Vol. 109, HY7, pp. 959-990.

15. Chang, H.H. (1988). Fluvial Processes in River Engineering, John Wiley and Sons, New York.

16. Chen, Y.H. and Simons, D.B. (1975). 'Mathematical modeling of alluvial channels,' Symp. on Modeling Techniques, Vol. I, 2nd Annual Symp. of Waterways, Harbors, and Coastal Eng. Div., ASCE, pp. 466-483.

17. Chow, V.T. (1959). Open-Channel Hydraulics, McGraw-Hill, New York.

18. Chow, V.T. (1964). Handbook of Applied Hydrology, Sections 7 and 25-II, McGraw-Hill, New York.

19. Chow, V.T., Maidment, D.R., and Mays, L.W. (1988). Applied Hydrology, McGraw-Hill, New York.

20. Colby, B.R. and Scott, C.H. (1965). 'Effects of water temperature on the discharge of bed material,' USGS Professional Paper 4626, U.S. Government Printing Office, Washington, DC.

21. Colon, R. and McMahon, G.F. (1987). 'BRASS model: Application to Savannah river system reservoirs,' Journal of Water Resources Planning and Management, ASCE. Vol. 113, No. 2, pp. 177-190.

22. Cooley, R.L. and Moin, S.A. (1976). 'Finite element solution of Saint-Venant equations,' J. Hydraul. Div., ASCE, Vol. 102, No. HY6, pp. 759-775.

23. Cunge, J.A. (1969). 'On the subject of a flood propagation computation method (Muskingum method),' J. Hydraul. Res., Vol. 7, No. 2, pp. 205-230.

24. Cunge, J.A. (1975b). 'Two-dimensional modeling of flood plains,' in Unsteady Flow in Open Channels, Vol. II, (Eds: K. Mahmood and V. Yevjevich), Chapter 17, pp. 705-762, Water Resources Publications, Fort Collins, Co.

25. Cunge, J.A., Holly, F.M., Jr., and Verway, A. (1980). Practical Aspects of Computational River Hydraulics, Pitman, Boston, Mass.

26. Danish Hydraulic Institute (1988). MIKE II Short Description, Horsholm, Denmark, 45 pp.

27. Davidson, D.D., and McCartney, B.L. (1975). 'Water waves generated by landslides in reservoirs,' J. Hydraul. Div., ASCE, Vol. 101, No. HY12, pp. 1489-1501.

28. Dawdy, D.R., Schaake, J.C., Jr., and Alley, W.M. (1978). Distributed Routing Rainfall-Runoff Model, U.S. Geological Survey Water Resources Investigations 78-90, 146 pp.

29. DeLong, L.L. (1986). 'Extension of the unsteady one-dimensional open-channel flow equations for flow simulation in meandering channels with flood plains,' Selected Papers in Hydrologic Science, U.S. Geological Survey Water Supply Paper 2220, pp. 101-105.

30. DeLong, L.L. (1989). 'Mass conservation: 1-D open channel flow equations,' J. Hydraul. Div., Vol. 115, No. 2, pp. 263-268.

31. Dooge, J.C.I. (1973). Linear Theory of Hydrologic Systems, Tech. Bul. No. 1468, USDA Agricultural Research Service, Beltsville, Md.

32. Dooge, J.C.I., Strupczewski, W.G., and Napiorkowski, J.J. (1982). 'Hydrodynamic derivation of storage parameters of the Muskingum model,' J. Hydrol., No. 54, pp. 371-387.

33. Dronkers, J.J. (1969). 'Tidal computations for rivers, coastal areas, and seas,' J. Hydraul. Div., ASCE, Vol. 95, No. HY1, pp. 29-77.

34. Engelund, K. and Hansen, E. (1983). A Monograph on Sediment Transport in Alluvial Streams, Teknisk Vorlog, Copenhagen, Denmark.

35. Franz, D.D. (1991). Unsteady flow solutions: FEQ/FEQUTL, Linsley, Krager Associates, Ltd., Mountain View, Cal.

36. Fread, D.L. (1971). 'Discussion of implicit flood routing in natural channels,' by M. Amein and C. S. Fang, J. Hydraul. Div., ASCE, Vol. 97, No. HY7, pp. 1156-1159.

37. Fread, D.L. (1973). 'Technique for implicit dynamic routing in rivers with tributaries,' Water Resources Research, Vol. 9, No. 4, pp. 918-926.

38. Fread, D.L. (1974). Numerical Properties of Implicit Four-Point Finite Difference Equations of Unsteady Flow, HRL-45, NOAA Tech. Memo NWS HYDRO-18, Hydrologic Research Laboratory, National Weather Service, Silver Spring, Md.

39. Fread, D.L. (1976). Theoretical Development of Implicit Dynamic Routing Model, HRL-113, Hydrologic Research Laboratory, National Weather Service, Silver Spring, Md.

40. Fread, D.L. (1977). 'The development and testing of a dam-break flood forecasting model,' Proc. of Dam-Break Flood Modeling Workshop, U.S. Water Resources Council, Washington, D.C., pp. 164-197.

41. Fread, D.L. (1978). 'NWS operational dynamic wave model,' Verification of Mathematical and Physical Models, Proceedings of 26th Annual Hydr. Div. Specialty Conf., ASCE, College Park, Md., pp. 455-464.

42. Fread, D.L. (1983). Applicability Criteria for Kinematic and Diffusion Routing Models, HRL-176, Hydrologic Research Laboratory, National Weather Service, Silver Spring, Md., 16 pp.

43. Fread, D.L. (1983). 'Computational extensions to implicit routing models,' Proceedings of the Conference on Frontiers in Hydraulic Engineering, ASCE, MIT, Cambridge, Mass., pp. 343-348.

44. Fread, D.L. (1985). 'Channel routing,' Hydrological Forecasting, (Eds: M.G. Anderson and T.P. Burt), John Wiley and Sons, New York, Chapter 14, pp. 437-503.

45. Fread, D.L. (1988). The NWS DAMBRK Model: Theoretical Background/User Documentation, HRL-256, Hydrologic Research Laboratory, National Weather Service, Silver Spring, Md., 315 pp.

46. Fread, D.L. (1989). 'Flood routing and the Manning n,' Proc. of the International Conference for Centennial of Manning's Formula and Kuichling's Rational Formula, (Ed: B.C. Yen), Charlottesville, Va., pp. 699-708.

47. Fread, D.L. (1989). 'National weather service models to forecast dam-breach floods,' Hydrology of Disasters (Eds: O. Starosolszky and O.M. Melder), Proc. of the World Meteorological Organization Technical Conference, November 1988, Geneva, Switzerland, pp. 192-211.

48. Fread, D.L. and Harbaugh, T.E. (1971). 'Open channel profiles by Newton's iteration technique,' J. Hydrol., Vol. 13, pp. 70-80.

49. Fread, D.L., and Lewis, J.M. (1988). 'FLDWAV: a generalized flood routing model,' Proc. of National Conference on Hydraulic Engineering, ASCE, Colorado Springs, Co., pp.668-673.

50. Fread, D.L., McMahon, G.F., and Lewis, J.L. (1988). 'Limitations of level-pool routing in reservoirs,' Proceedings, Third Water Resources Operations and Management Workshop, ASCE, Computational Decisions Support Systems for Water Managers, Fort Collins, Co.

51. Fread, D.L. and Smith, G.F. (1978). 'Calibration technique for 1-D unsteady flow models,' J. Hydraul. Div., ASCE, Vol. 104, No. HY7, pp. 1027-1044.

52. Freeze, R.A. (1972). 'Role of subsurface flow in generating surface runoff, 1. Base flow contributions to channel flow,' Water Resources Res., Vol. 8, No. 3, pp. 609-623.

53. Froehlich, D.C. (1987). 'Embankment-dam breach parameters,' Proc. of the 1987 National Conf. on Hydraulic Engr., ASCE, New York, August, pp. 570-575.

54. Garrison, J.M., Granju, J.P. and Price, J.T. (1969). 'Unsteady flow simulation in rivers and reservoirs,' J. Hydraul. Div., ASCE, Vol. 95, No. HY5, pp. 1559-1576.

55. Goodrich, R.D. (1931). 'Rapid calculation of reservoir discharge,' Civil Engineering, Vol. 1, pp. 417-418.

56. Gray, W.G., Pinder, G.F. and Brebbia, C.A. (1977). Finite Elements in Water Resources, Pentech Press, London.

57. Gunaratnam, D.J., and Perkins, F.E. (1970). 'Numerical solution of unsteady flows in open channels,' Report No. 127, Dept. of Civil Engr., MIT, Cambridge, Mass., 260 pp.

58. Harder, J.A. and Armacost, L.V. (1966). Wave Propagation in Rivers, Hydraulic Engng. Lab., Report 1, Series 8, Univ. of Cal. Berkeley, Cal.

59. Harley, B.M., Perkins, F.E., and Eagleson, P.S. (1970). A Modular Distributed Model of Catchment Dynamics, Report No. 133, R.M. Parsons Lab for Water Resources and Hydrodynamics, MIT, Cambridge, Mass.

60. Heijl, H.R. (1977). 'A method for adjusting values of Manning's roughness coefficient for floods in urban areas,' U.S. Geological Survey Journal of Research, Vol. 5, No. 5, pp. 541-595

61. Henderson, F.M. (1966). Open Channel Flow, Macmillan Co., New York, pp. 285-287.

62. Hinwood, J.B. and Wallis, I.G. (1975). 'Review of models of tidal waters,' J. Hydraul. Div., ASCE, Vol. 101, No. HY11, pp. 1405-1421.

63. Holly, F.M., Jr., Yang, J.C, Schwerz, P., Schaefer, J. Hsu, S.H., and Einhellig, R. (1990). CHARIMA-Numerical Simulation of Unsteady Water and Sediment in Multiple Connected Networks of Mobile-Bed Channels, University of Iowa, IIHR No. 343 Iowa City, Iowa.

64. Huber, W.C., Heany, J.P., Meding, M.A., Peltz, W.A., Sheikh, H., and Smith, G.F. (1975). Storm Water Management Model User's Manual, Nat. Environ. Res. Ctr. Document EPA-670/2-75-017, U.S. Environ. Protection Agency, Cincinnati, Ohio.

65. Hydrologic Engineering Center (1981). HEC-1 Flood Hydrograph Package - Users Manual, U.S. Army Corps of Engineers, Davis, Cal.

66. Hydrologic Engineering Center (1982). HEC-2 Water Surface Profiles Users Manual, U.S. Army Corps of Engineers, Davis, Cal.

67. Interagency Ad Hoc Sedimentation Work Group (1988). Twelve Selected Computer Stream Sedimentation Models Developed in the United States, Subcommittee on Sedimentation, Interagency Advisory Committee on Water Data, (S. Fan, ed.), published by the Federal Energy Regulatory Commission, U.S. Government Printing Office: 1989-250-618/00854, 552 pp.

68. Isaacson, E. and Keller, H.B. (1966). Analysis of Numerical Methods, John Wiley and Sons, New York.

69. Isaacson, E., Stoker, J.J., and Troesch, A. (1954). Numerical Solution of Flood Prediction and River Regulation Problems' Report II/III, No. IMM-NYU-205/235, New York Univ. Inst. of Math. Science, New York.

70. Jarrett, R.D. (1984). 'Hydraulics of high-gradient streams,' J. Hydraul. Div., ASCE, Vol. 110, No. HY11, Nov., pp. 1519-1539.

71. Johnson, B.H. (1974). Unsteady Flow Computations on the Ohio-Cumberland-Tennessee-Mississippi River System, Tech. Report H-74-8, U.S. Army Engineer Waterways Experiment Station, Vicksburg, Miss.

72. Johnson, B.H. (1982). Development of a Numerical Modeling Capability for the Computation of Unsteady Flow on the Ohio River and its Major Contributaries, Tech. Report HL-82-20, U.S. Army Engineer Waterways Experiment Station, Vicksburg, Miss.

73. Jones, S.B. (1981). 'Choice of space and time steps in the Muskingum-Cunge flood routing method,' Proc. of Instn. Civ. Engr., Part 2, No. 71, pp. 759-772.

74. Kalinin, G.P. and Miljukov, P.I. (1957). 'On the computation of unsteady flow in open channels,' Meteorologiya i Gidrologiya Zhuzurnal, Vol. 10, Leningrad, U.S.S.R.

75. Kamphuis, J.W. (1970). 'Mathematical tidal study of St. Lawrence River,' J. Hydraul. Div., ASCE, Vol. 96, No. HY3, pp. 643-664.

76. Keefer, T.N. and McQuivey, R.S. (1974). 'Multiple linearization flow routing model,' J. Hydraul. Div., ASCE, Vol. 100, No. HY7, pp. 1031-1046.

77. Koussis, A.D. (1978). 'Theoretical estimations of flood routing parameters,' J. Hydraul. Div., ASCE, Vol. 104, No. HY1, pp. 109-115.

78. Koutitas, C.G. (1977). 'Finite element approach to waves due to landslides,' J. Hydraul. Div., ASCE, Vol. 103, No. HY9, Sept., pp. 1021-1029.

79. Kouwen, N. (1988). 'Field estimation of the biomechanical properties of grass,' J. Hydraul. Res., Vol. 26, No. 5, pp. 559-568.

80. Krishnappan, B.G. (1979). 'Unsteady flow in mobile boundary channels,' Environ. Hydr. Sect., Hydr. Res. Div., National Water Res. Inst., Canada Centre for Inland Waters, Burlington, Ontario, 46 pp.

81. Kundzewicz, Z.W. (1984). 'Multilinear flood routing,' Acta Geophysica Polonica, Vol. 32, No. 4, pp. 419-445.

82. Lai, A.M.W. and Shen, H.T. (1991). 'Mathematical model for river ice process,' J. of Hydraul. Eng., ASCE, Vol. 117, No. 7, pp. 851-867.

83. Lai, Chintu (1986). 'Numerical modeling of unsteady open-channel flow,' Advances in Hydroscience, (V.T. Chow and B.C. Yen, eds.), Vol. 14, pp. 161-333, Academic Press, Orlando, Fla.

84. Leenderste, J.J. (1967). 'Aspects of a computational model for long-period water wave propagation,' Rand Report RM-5294-PR, Rand Corp. Santa Monica, Cal., 165 pp.

85. Leenderste, J.J. (1987). 'Aspects of SIMSYS2D, a system for two-dimensional flow computation,' Rand Report R-3572-USGS, Rand Corp., Santa Monica, Cal., 80 pp.

86. Li, R.M., Simons, D.B., and Stevens, M.A. (1975). 'Nonlinear kinematic wave approximation for water routing,' Water Resources Res., Vol. 11, No. 2, pp. 245-252.

87. Liggett, J.A. (1975). 'Basic equations of unsteady flow,' Unsteady Flow in Open Channels, Vol. I, (Eds: K. Mahmood and V. Yevjevich), Chapter 2, pp. 29-62, Water Resource Pub., Fort Collins, Co.

88. Liggett, J.A. and Cunge, J.A. (1975). 'Numerical methods of solution of the unsteady flow equations,' Unsteady Flow in Open Channels, Vol. I, (Eds: K. Mahmood and V. Yevjevich), Chapter 4, pp. 89-182, Water Resources Pub., Fort Collins, Co.

89. Liggett, J.A. and Woolhiser, D.A. (1967). 'Difference solutions of the shallow-water equations,' J. Engng. Mech. Div., ASCE, Vol. 95, No. EM2, pp. 39-71.

90. Lighthill, M.J. and Whitham, G.B. (1955). 'On kinematic floods -- flood movements in long rivers,' Proc., Royal Society, A220, London, pp. 281-316.

91. Linsley, R.K., Kohler, M.A., and Paulhus, J.L.H. (1986). Hydrology for Engineers, McGraw-Hill, New York, pp. 502-530.

92. McCarthy, G.T. (1938). 'The unit hydrograph and flood routing,' Conf. of the North Atlantic Div., U.S. Corps of Engineers, New London, Conn.

93. Meyer-Peter, E. and Muller, P. (1948). 'Formulas for bed-load transport,' Proc. of 2nd Congress IAHR, Paper No. 2, Stockholm, Sweden, pp. 39-64.

94. Miller, W.A. and Cunge, J.A. (1975). 'Simplified equations of unsteady flow,' Unsteady Flow in Open Channels, Vol. I, (Eds: K. Mahmood and V. Yevjevich), Chapt. 5, pp. 183-257, Water Resources Pub., Fort Collins, Co.

95. Miller, W.A. and Yevjevich, V. (1975). Unsteady Flow in Open Channels, Bibliography, Vol. III, Water Resources Pub. Fort Collins, Co.

96. Morris, H.M. and Wiggert, J.M. (1972). Applied Hydraulics in Engineering, The Ronald Press, New York.

97. Napiórkowski, J.J. and O'Kane, P. (1984). 'A new non-linear conceptual model of flood waves,' J. Hydrol., Vol. 69, No. 4, pp. 43-58.

98. Nash, J.E. (1957). 'The form of the instantaneous unit hydrograph,' International Association of Hydrological Sciences, No. 45, Vol. 3-4, pp. 114-121.

99. Nash, J.E. (1959). 'A note on the Muskingum method of flood routing,' J. Geophysical Res., Vol. 64, pp. 1053-1056.

100. Natale, T. and Todini, E. (1976). 'A stable estimator for linear models; 1. Theoretical developments and Monte Carlo experiments,' Water Resources Res., Vol. 12, No. 4, pp. 667-671.

101. Natural Environment Research Council (1975). Flood Studies Report, Vol. III, Flood Routing Studies, Inst. of Hydrology, Wallingford, England.

102. Nezhikhovskiy, R.A. (1964). 'Coefficients of roughness of bottom surface of slush ice cover,' Soviet Hydrology: Selected Papers, No. 2, pp. 127-148.

103. O'Brien, J.S. and Julien, P. (1984). 'Physical properties and mechanics of hyper-concentrated sediment flows,' Delineation of Landslide, Flash Flood, and Debris Flow Hazards in Utah, Utah State Univ., Utah Water Research Laboratory, Logan, Utah, (Ed: D.S. Bowles), General Series UWRL/G-85/03, pp. 260-279.

104. O'Donnell, T., Pearson, C., and Woods, R.A. (1988). 'Improved fitting for three parameter Muskingum procedure,' J. Hydraul. Div., ASCE, Vol. 114, No. 5, pp. 516-528.

105. Pariset, E., Hauser, R., and Gagnon, A. (1976). 'Formation of ice covers and ice jams in rivers,' J. Hydraul. Div., ASCE, Vol. 92, No. HY6, pp. 1-24.

106. Pogge, E.C. and Chiang, W.L. (1977). Further Development of a Stream-Aquifer System Model, Kansas Water Resources Research Inst., Univ. of Kansas, Lawrence, Kansas.

107. Ponce, V.M., Li, R.M., and Simons, D.B. (1978). 'Applicability of kinematic and diffusion models,' J. Hydraul. Div., ASCE, Vol. 104, No. HY3, pp. 353-360.

108. Ponce, V.M. and Yevjevich, V. (1978). 'Muskingum-Cunge method with variable parameters,' J. Hydraul. Div., ASCE, Vol. 104, No. HY12, pp. 1663-1667.

109. Preissmann, A. (1961). 'Propagation of translatory waves in channels and rivers,' in Proc., First Congress of French Assoc. for Computation, Grenoble, France, pp. 433-442.

110. Preissmann, A. and Cunge, J.A. (1961). 'Translatory wave calculations by computer,' Proc. of 9th Congress, IAHR, Dubrovnik, pp. 656-664.

111. Price, R.K. (1974). 'A comparison of four numerical methods for flood routing,' J. Hydraul. Div., ASCE, Vol. 100, No. HY7, pp. 879-899.

112. Price, R.K. (1977). FLOUT - A River Catchment Flood Model, Report IT168, Hydraulics Research Station, Wallingford, England.

113. Puls, L.G. (1928). Construction of Flood Routing Curves, House Document 185, U.S. 70th Congress, 1st session, Washington, D.C., pp. 46-52.

114. Rajar, R. (1978). 'Mathematical simultion of dam-break flow,' J. Hydraul. Div., ASCE, Vol. 104, No. HY7, pp. 1011-1026.

115. Rockwood, D.M. (1958). 'Columbia basin stream flow routing by computer,' Transactions, ASCE, Vol. 126, Part 4, pp. 32-56.

116. Saint-Venant, Barré de (1871). 'Theory of unsteady water flow, with application to river floods and to propagation of tides in river channels,' Computes rendus, Vol. 73, Acad. Sci., Paris, France, pp. 148-154, 237-240. (Translated into English by U.S. Corps of Engrs., No. 49-g, Waterways Experiment Station, Vicksburg, Miss., 1949.)

117. Samuels, P.G. (1985). Models of Open Channel Flow Using Preissmann's Scheme, Cambridge University, Cambridge, England, pp. 91-102.

118. Sayed, I. and Howard, D.C. (1983). 'Application of dynamic backwater modeling to Mactaquac headpond - Saint John River, N.B.,' Proceedings of 6th Canadian Hydrotechnical Conference, Canadian Society for Civil Engr., pp. 203-220.

119. Schaffranek, R.W. (1987). Flow Model for Open Channel Reach or Network, Professional Paper No. 1384, U.S. Geological Survey, 16 pp.

120. Schaffranek, R.W., Baltzer, R.A., and Goldberg, D.E. (1981). 'A model for simulation of flow in singular and interconnected channels,' Book 7, Automated Data Processing and Computations, TWRI Series, U.S. Geological Survey, Chapter C3, 110 p.

121. Shearman, J.O. (1990). Users Manual for WSPRO: A Computer Model for Water-Surface Profile Computations, Federal Highways Admin., Report No. FWHA/IP-89/027, 177 pp.

122. Singh, V.P. and McCann, R.C. (1980). 'Some notes on Muskingum method of flood routing,' J. Hydrol., Vol. 48, No. 3, pp. 343-361.

123. Slade, J.E., and Samuels, P.G. (1980). Modeling Complex River Networks, HR Pub. Paper No. 41, Hydraulics Research Limited, Wallingford, UK.

124. Smith, A.A. (1980). 'A generalized approach to kinematic flood routing,' J. Hydrol., Vol. 45, pp. 71-89.

125. Soil Conservation Service (1976). WSP2 Computer Program, Technical Release No. 61, Engineering Div., Soil Conservation Service, U.S. Dept. of Agriculture, 51 pp.

126. Stoker, J.J. (1953). Numerical Solution of Flood Prediction and River Regulation Problems; Derivation of Basic Theory and Formulation of Numerical Methods of Attack, Report I, No. IMM-NYU-200, New York Univ. Institute of Mathematical Science, New York.

127. Stoker, J.J. (1957). Water Waves, Interscience, New York, pp. 452-455.

128. Streeter, V.L. and Wylie, E.B. (1967). Hydraulic Transients, McGraw Hill, New York, pp. 239-259.

129. Strelkoff, T. (1969). 'The one-dimensional equations of open-channel flow,' J. Hydraul. Div., ASCE, Vo. 95, No. HY3, pp. 861-874.

130. Strelkoff, T. (1970). 'Numerical solution of Saint-Venant equations,' J. Hydraul. Div., ASCE, Vol. 96, No. HY1, pp. 223-252.

131. Strelkoff, T. and Katopodes, N.D. (1977). 'Border irrigation hydraulics with zero inertia,' J. Irrig./Drain. Div., ASCE, Vol. 103, pp. 325-342.

132. Task Committee on Bed Configuration and Hydraulic Resistance of Alluvial Streams (1974). The Bed Configuration and Roughenss of Alluvial Streams, Committee on Hydraulics and Hydraulic Eng., The Japan Society of Civil Engr.

133. Todini, E. and Bossi, A. (1985). PAB (Parabolic and Backwater) -- An Unconditionally Stable Flood Routing Scheme Particularly Suited for Real Time Forecasting and Control, Pub. n.1, Univ. di Bologna, Bologna, Italy.

134. Toffalleti, F.B. (1969). 'Definitive computations of sand discharge in rivers,' J. Hydraul. Div., ASCE, Vol. 95, No. HY1, pp. 225-246.

135. U.S. Army Corps of Engineers (1969). 'Missouri River channel regime studies, Omaha Distict,' Missouri River Div. Sediment Series 13B, Omaha, Neb.

136. Uzuner, M.S. (1975). 'The composite roughness of ice-covered streams,' J. Hydraul. Res., Vol. 13, No. 1, pp. 79-102.

137. Vasiliev, O.F., Gladyshev, M.J., Pritvits, N.A., and Sudobicher, V.G. (1965). 'Methods for the calculation of shock waves in open channels,' Proc., IAHR Eleventh Int'l. Congress, Vol. 44, No. 3, Leningrad, U.S.S.R.

138. Verwey, A. and Haperen, M.J.M. (1988). 'HD-system RUBICON -- a user-friendly package for the simulation of unsteady flow in open channel networks,' Hydrosoft, Vol. 1, No. 1, pp. 3-12.

139. Viessman, W., Jr., Knapp, J.W., Lewis, G.L., and Harbaugh, T.E. (1977). Introduction to Hydrology, 2nd ed., Intext Educational Publishers, New York.

140. Walton, R., and Christensen, B.A. (1980). 'Friction factors in storm-surges over inland areas,' J. Waterway, Port, Coastal and Ocean Div., ASCE, Vol. 106, WW2, pp. 261-271.

141. Wormleaton, P.R. and Karmegam, M. (1984). 'Parameter optimization in flood routing,' J. Hydraul. Div., ASCE, Vol. 110, No. HY12, pp. 1789-1814.

142. Yang, C.T. (1972). 'Unit stream power and sediment transport,' J. Hydraul. Div., ASCE, Vol. 18, No. HY10, pp. 1805-1826.

143. Yapa, P.D. and Shen, H.T. (1986). 'Unsteady flow simulation for an ice-covered river,' J. Hydr. Div., ASCE, Vol. 112, No. 11, pp. 1036-1049.

Table 10.2.1 Lumped Flow Routing Methods

Model Type	Name	References
Level-Pool	Puls, Goodrich	17,18,44,55,61,91,94,113
Level-Pool	Modified Puls	65
Level-Pool	Runge-Kutta	19
Level-Pool	Iterative Trapezoidal Integration	40,45
Storage Routing	Kalinin-Miljukov	31,44,74,77,94
Storage Routing	Lag and Route	44,91
Storage Routing	Muskingum	17,18,19,32,44,91,92,94,96,104,122,139
Storage Routing	SSARR	94,115
Storage Routing	Tatum	44
Linear Systems	Linear Reservoir	19,31,44,98
Linear Systems	SOSM	97
Linear Systems	Linearized St. Venant	90
Linear Systems	Multiple Linearized	76,81
Linear Systems	CLS	100

Table 10.3.1 One-Dimensional Distributed Flow Routing Models

Model Type	Name	Reference(s)	Finite-Difference Scheme	Special Features	Availability
Dynamic	BRANCH	119,120	4I	b,d,e,g,i,j	NP
Dynamic	BRASS	21	4I	a,d,e,f,g,i,j,n,r	NP
Dynamic	CARIMA (ONDYN)	25	4I	b,d,e,f,i,j	P
Dynamic	CHARIMA	63	4I	b,d,e,h,i,j	NP
Dynamic	DAMBRK	19,40,45,47	4I	c,d,e,f,i,j,k,m	NP
Dynamic	DWOPER	19,37,41	4I	b,d,e,f,g,i,j,l	NP
Dynamic	EXTRAN	64	E	a,d,l,n,p	NP
Dynamic	FEQ	35	4I	b,d,e,f,i,j,n,l	NP
Dynamic	FLDWAV	19,44,49	4I	b,c,d,e,f,g,h,i,j,k,l,m	NP
Dynamic	FLOSED	72	4IL	a,d,h,i	NP
Dynamic	FLUVIAL	15	4I	h,i	P
Dynamic	LORIS	123	4I	b,d,e,f,i,j	P
Dynamic	MOBED	80	4IL	h,i,j	NP
Dynamic	RICE	82,143	4I	j,q	P
Dynamic	RUBICON	138	4I	b,d,e,f,h,i,j,l	P
Dynamic	SOC/SOCJM	54,71	E	a,i	NP
Dynamic	S11	4,26	6I	b,c,d,e,f,h,i,j,k,l,n,p	P
Dynamic	UNET	11	4IFL	b,d,e,f,i,j	P
Diffusion	Muskingum-Cunge	15,19,23,44,94,101,108,112	4P	a,c,j	NP
Diffusion	PAB	133	CI/FB	b,c,f,h,j,n,p	NP
Diffusion	Zero-Inertia	58,131	E		NP
Kinematic	HEC-1	65	E	k,n	NP
Kinematic	MITCAT	59	E	n	NP
Kinematic	Nonlinear	86,124	4I		NP

Legend

NP - nonproprietary
P - proprietary
4I - weighted 4-point nonlinear implicit
4IL - weighted 4-point linear implicit
4IFL - fully forward 4-point linear implicit
6I - 6-point linear implicit; optional iteration
E - explicit
4P - linear/nonlinear 4-point
CI/FB - convolution integral (flow)/finite dif. backwater eq. (depth)

Special Features

a - dendritic system of interconnecting channels
b - dendritic/looped system of interconnecting channels
c - subcritical/supercritical mixed flow
d - assortment of external and internal boundaries
e - special treatment of floodplains
f - special treatment for overtopping of levees
g - automatic calibration of variable friction coefficient
h - sediment transport (mobile-bed) effects
i - dead storage effects
j - variable friction
k - dam-break flood generation
l - storm sewer capabilities including pressurized flow
m - non-Newtonian (mud) flow capabilities
r - reservoir operations

Table 10.3.2 Internal Boundary Conditions

Type of Boundary	Equation	
Critical Flow	$Q_i = \sqrt{g/B}\ A^{3/2}$	(17,44,61)
Dam		
Discharge Hydrograph	$Q_i = Q(t)$	
Stage Hydrograph	$h_i = h(t)$	
Rating Curve	$Q_i = K_b Q_b + K_s Q_s + Q_g + K_{cs} Q_{cs} + Q_t$	(44,45)
Breach Flow	$Q_v = 3.1b\,(h - h_{br})^{3/2} + 2.45z\,(h - h_{br})^{5/2}$	(44,45,47)
Spillway Flow	$Q_s = C_s L_s\,(h - h_s)^{3/2}$	
Gate Flow	$Q_g = \sqrt{2g}\ C_g A_g\,(h - \hat{h})^{1/2}$ where $\hat{h} = h_g$ if $h_t \le h_g$; $\hat{h} = h_t$ if $h_t > h_g$	(44,45)
Dam Crest Flow	$Q_{cs} = C_d L_d\,(h - h_d)^{3/2}$	
Turbine Flow	$Q_t = Q(t)$	
Bridge	$Q_i = Q_{bo} + K_{em} Q_{em} + K_b Q_b$	(45)
Bridge Flow	$Q_{bo} = \sqrt{2g}\ C_b A_b \left[h - h_t + (Q/A)^2/2g\right]^{1/2}$	(45)
Embankment Flow	$Q_{em} = C_{em} L_{em}\,(h - h_{em})^{3/2}$	(45)

where: A, A_g, A_b = wetted cross-sectional area, area of gate opening, wetted area of bridge opening

b = instantaneous bottom breach width = $b_o\,(t_{br}/\tau_{br})$ for $t_{br} \le \tau_{br}$; otherwise $b = b_o$ (45,47)

b_o = final bottom breach width, ft = $14.3\,(V_r h_d)^{0.25} - 0.5\,z h_d$ (45,47,53)

C_s, C_d, C_{em}, C_g = discharge coefficients for spillway, dam overtopping, embankment, bridge, or gate flow

h = elevation of water at the upstream side of structure

h_{br} = breach bottom elevation

h_d = top of dam elevation

h_s, h_g, h_{em} = elevation of spillway crest, centerline of gate opening, top of embankment

h_t = tailwater elevation

K_b, K_s, K_{cs}, K_{em} = submergence correction factor for breach, spillway, dam overtopping, bridge embankment overflow

L_s, L_d, L_{em} = length of spillway, dam, embankment

Q_b, Q_{bo}, Q_{cs}, Q_{em}, Q_g, Q_i, Q_s, Q_t = discharge (breach, bridge opening, crest overflow, embankment overflow gate, internal boundary, spillway, turbine)

t_{br} = time since beginning of breach formation, hrs.

τ_{br} = formation of time of breach, hrs = $0.6\,V_r^{0.47}/h_d^{0.9}$ (45,47,53)

V_r = volume of reservoir, acre-ft

z = side slope of breach, l:vertical to z:horizontal

Table 10.4.1 Data Used in Lumped and Distributed Routing Models

Data Type	Routing Models	
	Lumped	Distributed
Observed Inflow Hydrograph, I(t)	a	c
Observed Outflow Hydrograph, Q(t)	a	c
Observed Water-Surface Elevation Time Series, h(t)	-	c
Lateral Inflow Hydrograph, q(t)	-	d
Surface Area -- Elevation Table, Sa(h)	b	-
Cross-Section Topwidth -- Elevation Table, B(h)	-	e
Friction Coefficient -- Water-Surface Elevation or Discharge Table, n(h or Q)	-	f
Expansion/Contraction Coefficients, K_{ec}	-	g
Sinuosity Factors, s_c and s_m	-	h

a - required for calibration of storage and linear systems models
b - required for level-pool model
c - required for calibration
d - not always required
e - always required
f - can be obtained via calibration
g - can be assumed 0.0 for fairly uniform channels
h - can be assumed 1.0 for fairly straight channels

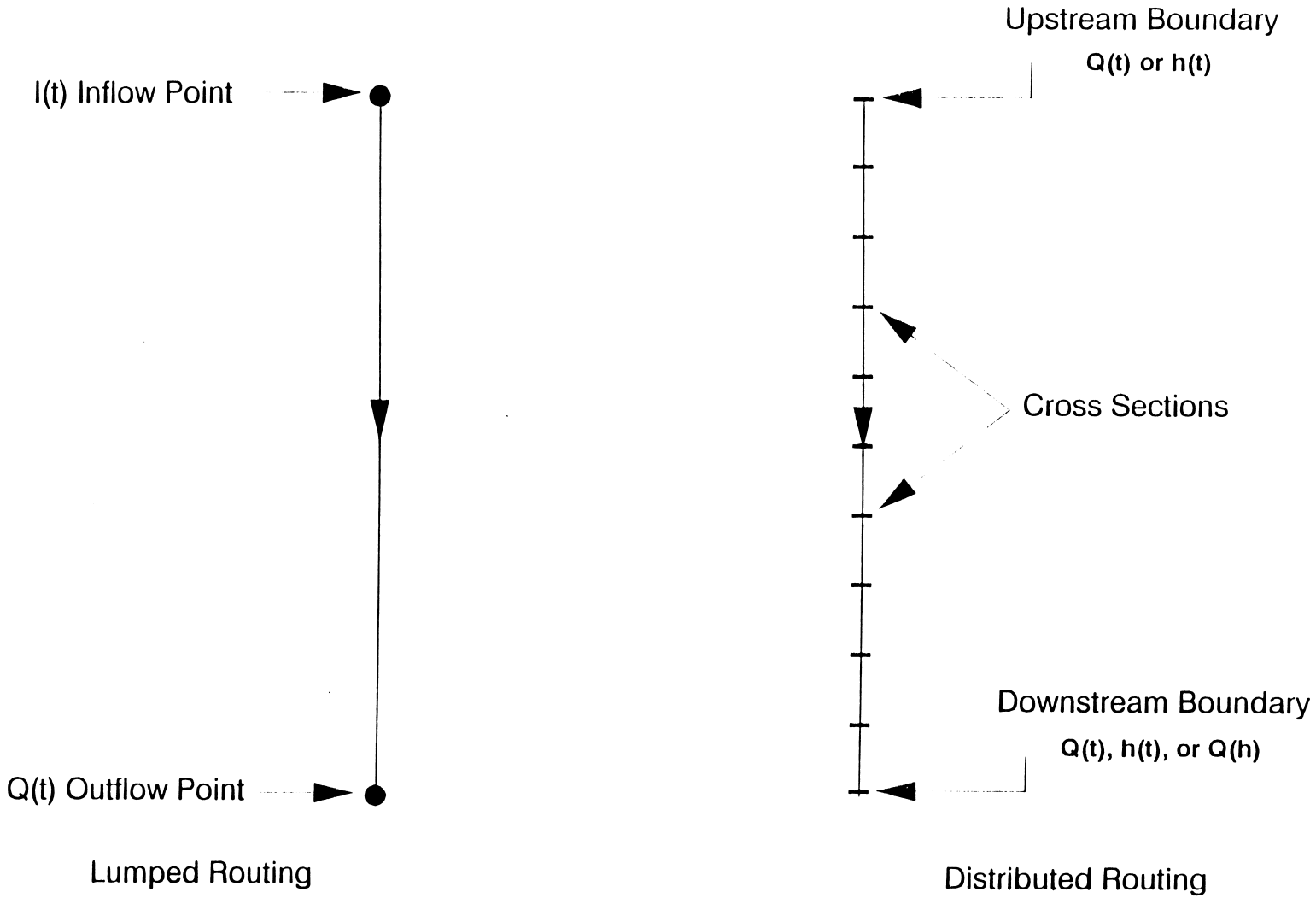

Fig. 10.1.1. Schematic showing lumped and distributed flow routing systems, where Q is discharge or flow rate, and h is water surface elevation or stage.

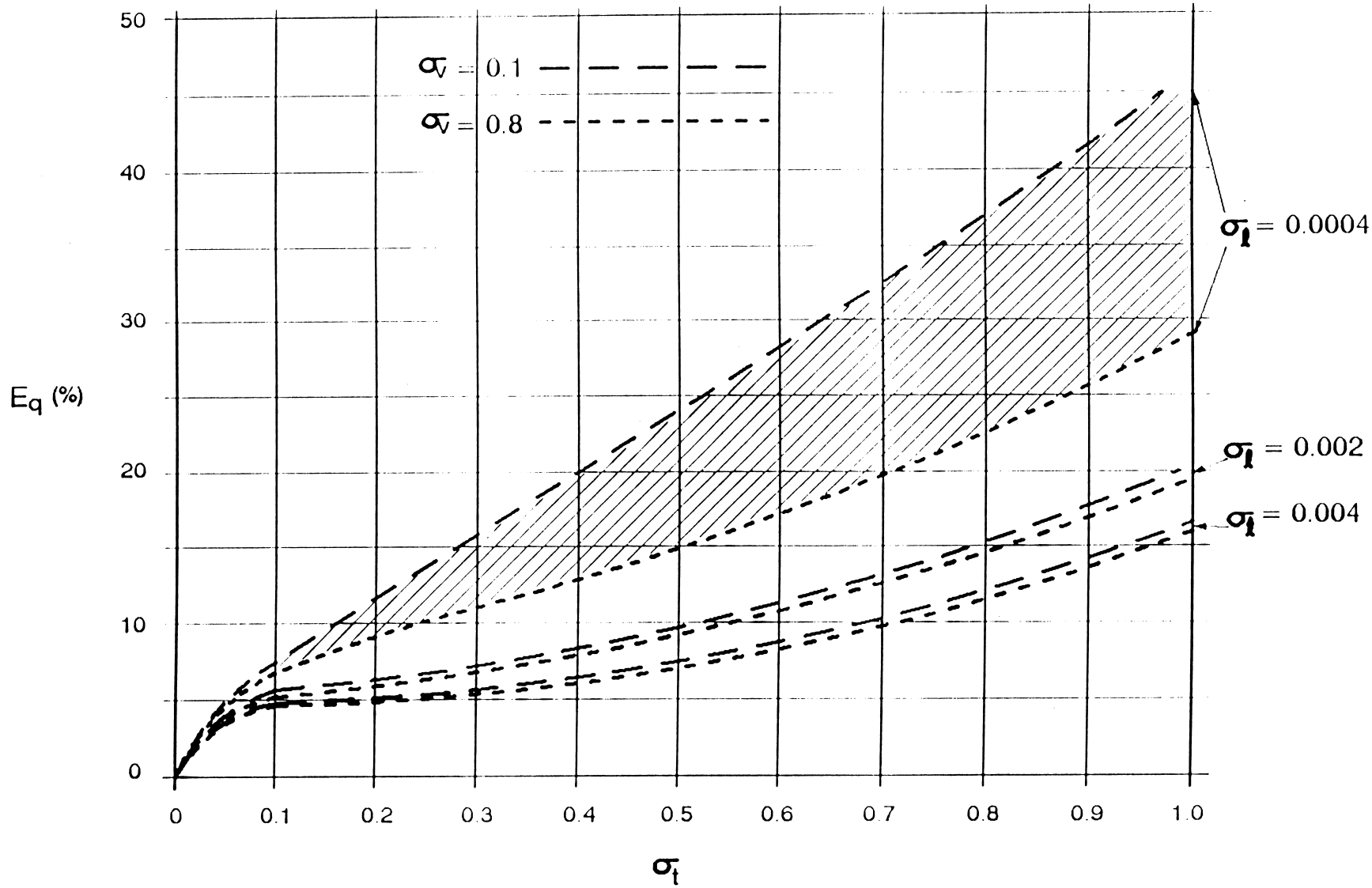

Fig. 10.1.2 Level-pool routing compared to dynamic routing showing the normalized error (E_q) of the rising limb of the outflow hydrograph as a function of σ_t, σ_l and σ_v (dimensionless parameters that reflect the reservoir volume, length, depth, and the inflow hydrograph volume and time of rise.)

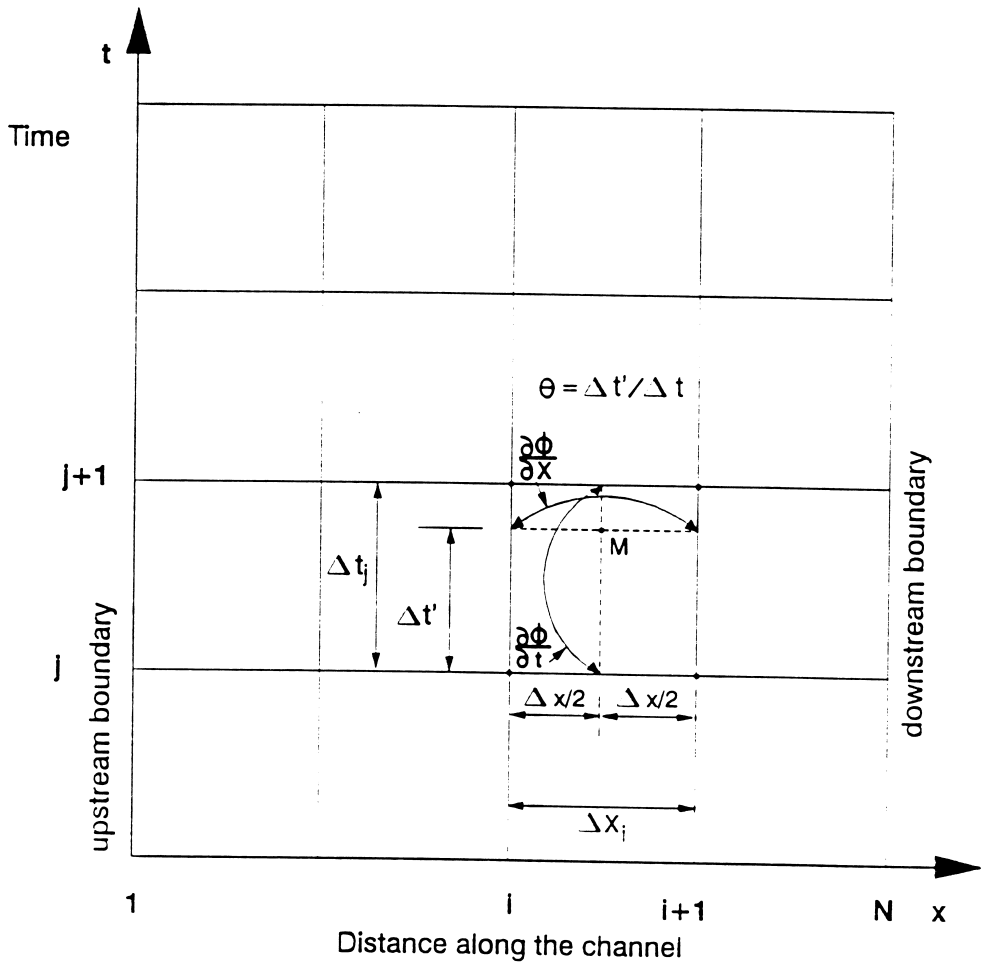

Fig. 10.3.1 The x-t solution domain showing weighted four-point implicit scheme.

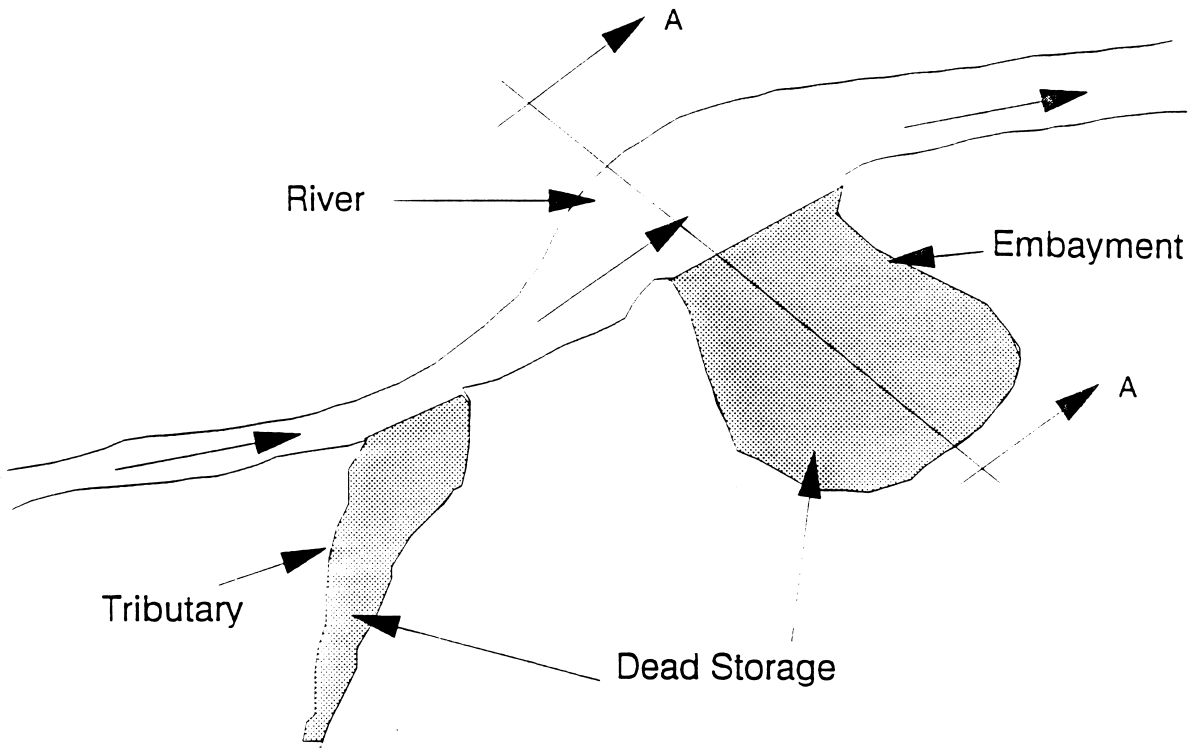

Plan View

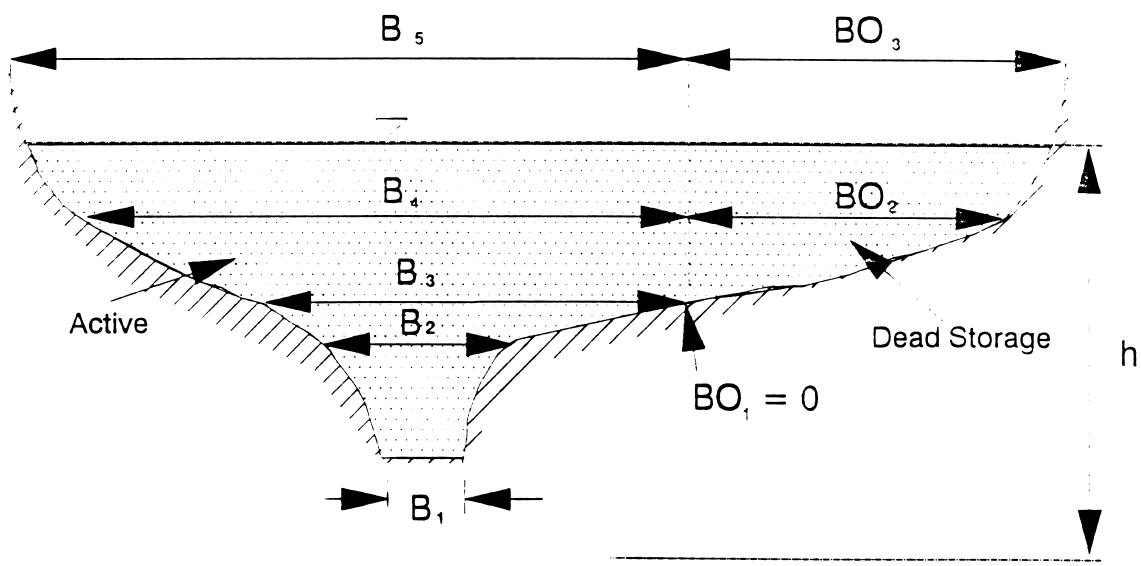

Cross Section A-A

Fig. 10.4.1. Plan view of river with active and dead storage areas, and cross section view.